C-ADAPTER: ADAPTING DEEP CLASSIFIERS FOR EFFICIENT CONFORMAL PREDICTION SETS

Anonymous authors
Paper under double-blind review

ABSTRACT

Conformal prediction, as an emerging uncertainty quantification technique, typically functions as post-hoc processing for the outputs of trained classifiers. To optimize the classifier for maximum predictive efficiency, Conformal Training rectifies the training objective with a regularization that minimizes the average prediction set size at a specific error rate. However, the regularization term inevitably deteriorates the classification accuracy and leads to suboptimal efficiency of conformal predictors. To address this issue, we introduce **Conformal Adapter** (C-Adapter), an adapter-based tuning method to enhance the efficiency of conformal predictors without sacrificing accuracy. In particular, we implement the adapter as a class of intra order-preserving functions and tune it with our proposed loss that maximizes the discriminability of non-conformity scores between correctly and randomly matched data-label pairs. Using C-Adapter, the model tends to produce extremely high non-conformity scores for incorrect labels, thereby enhancing the efficiency of prediction sets across different coverage rates. Extensive experiments demonstrate that C-Adapter can effectively adapt various classifiers for efficient prediction sets, as well as enhance the conformal training method.

1 INTRODUCTION

Quantifying the uncertainty of predictions is critical for artificial intelligence systems, particularly in high-stakes environments (e.g., financial decision-making and medical diagnostics). Conformal prediction, a statistic framework for uncertainty estimation, converts an algorithm's predictions into prediction sets containing the true class with a user-specified coverage rate (Balasubramanian et al., 2014; Shafer & Vovk, 2008). Critically, the validity of sets is satisfied in a distribution-free sense: they possess explicit, non-asymptotic guarantees even without distributional assumptions or model assumptions. To obtain informative outputs, it is of great importance to improve the *efficiency* of conformal predictors, aiming for the prediction sets with minimal ambiguity (Sadinle et al., 2019).

Conformal prediction typically functions as post-hoc processing for the output of trained classifiers, which might already be either unnecessarily conservative or overconfident (Bellotti, 2021; Stutz et al., 2021). To optimize the predictive efficiency, Conformal Training (Stutz et al., 2021) rectifies the training objective with a regularization that minimizes the average prediction set size at a specific error rate (e.g., 0.01). However, the regularization term inevitably deteriorates the classifier accuracy by increasing the difficulty of converging to an optimal solution (Stutz et al., 2021), which in turn leads to the suboptimal efficiency of the conformal predictor. This challenge is especially significant when dealing with many classes, making it difficult to apply to large-scale datasets such as ImageNet (Deng et al., 2009). This motivates our methodology, which enables the efficient adaptation of trained classifiers for conformal prediction without sacrificing classification accuracy.

In this work, we propose *Conformal Adapter* (dubbed **C-Adapter**), an adapter-based tuning method to enhance the efficiency of conformal predictors. In particular, we tune an adapter layer appended to trained classifiers for conformal prediction using the training data. Our key idea is to adapt trained classifiers for conformal prediction while preserving the ranking of labels in the output logits, thereby maintaining the top-k accuracy of the classifiers. To achieve this, we implement the adapter as a class of intra order-preserving functions (Rahimi et al., 2020). For the optimization of this adapter, we propose a loss function that enhances the discriminability of non-conformity scores between correctly and randomly matched data-label pairs. In effect, the loss encourages the non-conformity scores of correctly matched data-label pairs to be lower than those of incorrectly matched ones, resulting in more efficient predictions across different coverage rates. Equipped with C-Adapter, the predictor maintains top-k accuracy and generates highly efficient prediction sets. For better clarity, we include a diagram in Appendix C to visually illustrate the application of C-Adapter.

To validate our method, we conduct extensive evaluations on three benchmarks of image classification, including CIFAR-100 (Krizhevsky et al., 2009), ImageNet (Deng et al., 2009), and ImageNet-V2 (Recht et al., 2019). The results demonstrate that C-Adapter can significantly enhance the efficiency of conformal predictors. For example, C-Adapter reduces the average size for APS from 9.21 to 2.86 on ImageNet (Deng et al., 2009) with DenseNet121 (Huang et al., 2017) at $\alpha = 0.1$. This approach also generalizes effectively to different score functions, consistently improving their efficiency. Moreover, C-Adapter can enhance the efficiency of prediction sets while simultaneously improving their conditional coverage. Notably, our method is easy to implement in practice, as it does not require heavy tuning of hyperparameters and incurs low computational costs.

We summarize our contributions as follows:

- We propose C-Adapter, a simple and effective method to enhance the efficiency of conformal predictors without sacrificing classifier accuracy. This approach serves as a distinctive complement to existing score-based and training-based conformal prediction algorithms.
- We theoretically demonstrate that enhancing the discriminability of non-conformity scores between correctly and randomly matched data-label pairs is equivalent to improving the overall efficiency of conformal predictors. To this end, we propose a loss function specifically designed to achieve this goal and apply it to optimize our conformal adapter.
- We empirically show that C-Adapter effectively adapts various classifiers for efficient prediction sets across different non-conformity score functions. Moreover, we validate that C-Adapter outperforms Conformal Training and can further enhance its performance.

2 BACKGROUND

Setup In this work, we consider the multi-class classification task with K classes. Let $(X, Y) \sim \mathcal{P}_{\mathcal{X}\mathcal{Y}}$ denote a random data pair sampled from the joint distribution $\mathcal{P}_{\mathcal{X}\mathcal{Y}}$, where $\mathcal{X} \subset \mathbb{R}^d$ is the input space and $\mathcal{Y} := \{1, \cdots, K\}$ is the label space. Given a training set, we learn a classifier $f : \mathcal{X} \to \mathbb{R}^K$ with parameter $\boldsymbol{\theta}$. Given an instance $\boldsymbol{x}$, we predict the probability of class k by:

$$\hat{\pi}_k(\boldsymbol{x}; \boldsymbol{\theta}) = \psi(f_k(\boldsymbol{x}; \boldsymbol{\theta})) = \frac{e^{f_k(\boldsymbol{x}; \boldsymbol{\theta})}}{\sum_{i=1}^{K} e^{f_i(\boldsymbol{x}; \boldsymbol{\theta})}}, \tag{1}$$

where ψ denotes the softmax function and $f_k(\boldsymbol{x}; \boldsymbol{\theta})$ is the k-th element of the logits $f(\boldsymbol{x}; \boldsymbol{\theta})$. Deep classifiers usually suffer from the miscalibration issue: the estimated probabilities might be either conservative or overconfident, leading to inaccurate assessments of uncertainty (Guo et al., 2017).

Conformal Prediction In uncertainty quantification, conformal prediction (Vovk et al., 2005) seeks to construct prediction sets $\mathcal{C}(X) \subseteq \mathcal{Y}$ such that $\mathbb{P}\{Y \in \mathcal{C}(X)\} \geq 1 - \alpha$ for a pre-specified error rate $\alpha \in (0, 1)$. To satisfy the desired coverage rate $1 - \alpha$, we take an independent conformal calibration dataset $\mathcal{D}_{\text{cal}} := \{(\boldsymbol{x}_i, y_i)\}_{i=1}^n$, and then determine the threshold τ_α such that the prediction sets are large enough to achieve the desired coverage level of $1 - \alpha$ on this calibration set. Specifically, we calculate the non-conformity score $s_i := S(\boldsymbol{x}_i, y_i; \hat{\pi})$ for each sample $(\boldsymbol{x}_i, y_i)$ in the calibration set where S is a pre-specified score function to measure non-conformity of each input sample. We then determine the threshold τ_α as the $1 - \alpha$ quantile of the set $\{s_i\}_{i=1}^n$, as follows:

$$\tau_\alpha = \inf \left\{ s : \frac{|\{i \in \{1, \cdots, n\} : s_i \leq s\}|}{n} \geq \frac{\lceil (n+1)(1-\alpha) \rceil}{n} \right\}.$$

During testing, we calculate the non-conformity score $S(\boldsymbol{x}_{n+1}, y; \hat{\pi})$ for a given instance $\boldsymbol{x}_{n+1}$ and each label $y \in \mathcal{Y}$. Then, the prediction set $\mathcal{C}(\boldsymbol{x}_{n+1}; \tau_\alpha, \hat{\pi})$ with $1 - \alpha$ coverage is constructed by:

$$\mathcal{C}(\boldsymbol{x}_{n+1}; \tau_\alpha, \hat{\pi}) := \{y \in \mathcal{Y} : S(\boldsymbol{x}_{n+1}, y; \hat{\pi}) \leq \tau_\alpha\}. \tag{2}$$

In other words, the final prediction sets achieve *marginal coverage* by containing all labels with non-conformity scores below the threshold (Vovk, 2012; Angelopoulos et al., 2020). In addition

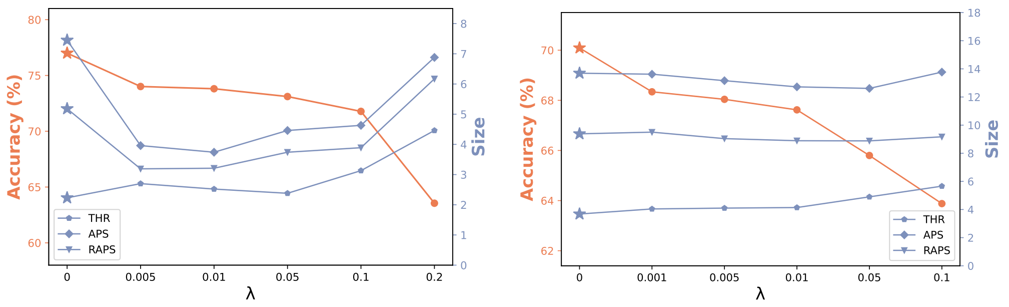

(a) CIFAR-100

(b) ImageNet

Figure 1: **The accuracy and efficiency of ConfTr with various $\boldsymbol{\lambda}$**, using THR, APS and RAPS at $\alpha = 0.1$. The experiments are conducted with ResNet18 on (a) CIFAR-100 and (b) ImageNet. ★ represents the baseline without ConfTr. The findings indicate that the increment of λ decreases the classification accuracy, ultimately leading to suboptimal efficiency in conformal prediction.

to the coverage, we typically expect to optimize the size of prediction sets, which is referred to as *efficiency*. Nevertheless, the length of the resulting prediction sets can vary dramatically depending on the design of $S(\boldsymbol{x}, y; \hat{\pi})$. In this work, we consider three popular score functions for classification, including THR (Sadinle et al., 2019), APS (Romano et al., 2020), and RAPS (Angelopoulos et al., 2020). We provide a detailed introduction to these score functions in Appendix B.1.

Conformal Training Conformal prediction typically works as post-hoc processing for the outputs of trained classifiers. To optimize the classifier for maximum predictive efficiency, Conformal Training (ConfTr) (Stutz et al., 2021) rectifies the training objective with a regularization that minimizes the average prediction set size at a specific error rate α. The loss function is formulated as:

$$\mathcal{L}_{\text{ConfTr}}(f(\boldsymbol{x};\boldsymbol{\theta}), y, \tau_{\alpha}^{\text{soft}}) = \mathcal{L}_{\text{cls}}(f(\boldsymbol{x};\boldsymbol{\theta}), y) + \lambda \mathcal{L}_{\text{size}}(f(\boldsymbol{x};\boldsymbol{\theta}), \tau_{\alpha}^{\text{soft}}), \tag{3}$$

Here, $\mathcal{L}_{\text{cls}}$ represents the classification loss, while $\mathcal{L}_{\text{size}}$ refers to the size loss, which approximates the size of the prediction set at a coverage rate of $1-\alpha$. Here, $\tau_{\alpha}^{\text{soft}}$ denotes the soft threshold and λ controls the strength of the regularization term. We provide a detailed introduction to ConfTr in Appendix B.2. Notably, while ConfTr with a tuned hyperparameter λ may improve the efficiency of conformal predictors, the regularization term $\mathcal{L}_{\text{size}}$ inevitably deteriorates the accuracy of the classifier by increasing the difficulty of converging to an optimal solution (Stutz et al., 2021).

To provide a straightforward view, we demonstrate the effect of the regularization term $\mathcal{L}_{\text{size}}$ on the accuracy and efficiency of conformal predictors in Figure 1. We conduct experiments of ConfTr with various λ, using ResNet18 on CIFAR100 and ImagNet. The results demonstrate that using this regularization continuously degrades the classification accuracy of the classifier as λ increases. For efficiency, ConfTr raises the average size of APS and RAPS after achieving the optimal performance on CIFAR-100. On ImageNet, ConfTr offers only marginal benefits for the efficiency of conformal predictors. The negative effect of ConfTr is especially noticeable on THR: the average size of THR is consistently increased over various λ. The decrease in classification accuracy inevitably results in larger prediction sets, which in turn limits the efficiency on average. We present a detailed description of the experimental setup and the effect of the regularization term $\mathcal{L}_{\text{size}}$ on top-k classification accuracy in Appendix H.1. We proceed by introducing our method, targeting this issue.

3 METHOD

In our previous analysis, we demonstrate that ConfTr deteriorates the classification accuracy, thereby hindering the efficiency of conformal predictors. To address this issue, our key idea is to adapt the trained classifiers for conformal prediction while preserving the ranking of labels in the output logits, thereby keeping the top-k accuracy of the original classifier unchanged.

Conformal Adapter To this end, we propose a novel adapter-based tuning method – *Conformal Adapter* (dubbed **C-Adapter**), which appends an adapter layer to trained classifiers for conformal prediction. Formally, we use $g: \mathbb{R}^K \to \mathbb{R}^K$ to denote the conformal adapter that takes the model

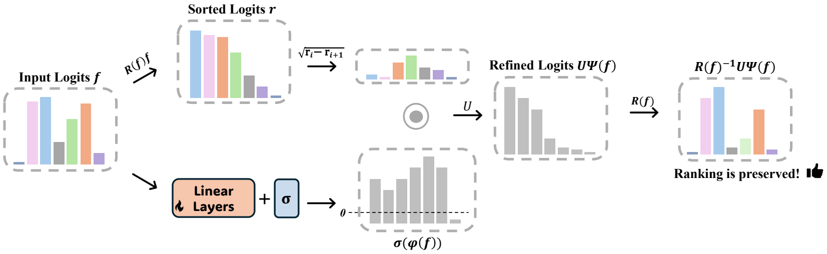

Figure 2: **Flow of C-Adapter.** The design follows the definition of intra order-preserving functions (Rahimi et al., 2020, Theorem 1), ensuring that the refined logits maintain the ranking of the inputs.

outputs $f(\boldsymbol{x};\boldsymbol{\theta})$ as input. Then, the final prediction of the model equipped with C-Adapter is:

$$\widetilde{\pi}(\boldsymbol{x};\boldsymbol{\theta},\boldsymbol{w}) = \psi(g(f(\boldsymbol{x};\boldsymbol{\theta});\boldsymbol{w})),$$

where $\boldsymbol{w}$ denotes the parameters of C-Adapter. While ConfTr alters the parameters of trained classifiers $\boldsymbol{\theta}$ through retraining or fine-tuning, we only update a few trainable parameters $\boldsymbol{w}$ added for conformal prediction. In addition to enhancing training efficiency, the adapter-based tuning method requires access only to the model outputs. This makes it compatible with black-box models (e.g., online APIs) and other modern neural networks (e.g., Radford et al. (2021, CLIP)).

Importantly, the adapter requires to be learned within a hypothesis space that can provably guarantee preserving the accuracy of the original network f. To achieve that, we implement the adapter as a class of *intra order-preserving functions* (Rahimi et al., 2020), a family of functions that is both necessary and sufficient to keep the top-k accuracy of the original network unchanged. Formally, a function $h : \mathbb{R}^K \to \mathbb{R}^K$ is *intra order-preserving*, if, for all $i, j \in [K]$ and any vector $\boldsymbol{x} \in \mathbb{R}^K$, $\boldsymbol{x}_i > \boldsymbol{x}_j$ (or $\boldsymbol{x}_i = \boldsymbol{x}_j$) if and only if $h_i(\boldsymbol{x}) > h_j(\boldsymbol{x})$ (or $h_i(\boldsymbol{x}) = h_j(\boldsymbol{x})$). For convenience, we use $\boldsymbol{f}$ to indicate the model output $f(\boldsymbol{x};\boldsymbol{\theta})$. We denote $R : \mathbb{R}^K \to \mathbb{U}^K$ as the sorting function, where $\mathbb{U}^K \subset \{0,1\}^{K\times K}$ represents the set of $K \times K$ permutation matrices. We have $\boldsymbol{r} = R(\boldsymbol{f})\boldsymbol{f}$ as the sorted $\boldsymbol{f}$, satisfying $\boldsymbol{r}_1 > \cdots > \boldsymbol{r}_K$. We use U to denote the $K \times K$ upper-triangular matrix of ones.

To ensure that C-Adapter belongs to the class of *intra order-preserving functions*, we define it by

$$g(\boldsymbol{f};\boldsymbol{w}) = R(\boldsymbol{f})^{-1}U\Psi(\boldsymbol{f}),$$

where the i-th term of $\Psi(\boldsymbol{f})$ is formulated as:

$$\Psi_i(\boldsymbol{f}) = \begin{cases} \sqrt{(\boldsymbol{r}_i - \boldsymbol{r}_{i+1})}\sigma(\varphi_i(\boldsymbol{f})) & \text{for } i < K, \\ \varphi_K(\boldsymbol{f}) & \text{for } i = K. \end{cases}$$

Here, $\varphi(\boldsymbol{f}) = \boldsymbol{w} \cdot \boldsymbol{f} + \boldsymbol{w}'$, and σ represents the sigmoid function. We denote $\varphi_i(\boldsymbol{f})$ as the i-th component of $\varphi(\boldsymbol{f})$. We outline the workflow in Figure 2. Since $\Psi(\boldsymbol{f})$ is continuous in $\boldsymbol{f}$, it is straightforward to verify that this structure satisfies the requirements of the intra order-preserving family (Rahimi et al., 2020, Theorem 1). The core idea is to decouple the label ranking and the logit values in the tuning. It begins by preserving a duplicate of the label ranking, and then transmit the logits to the linear layer for processing. Finally, we recover the label ranking in the output. We provide a more detailed description of this function family in Appendix D. This structure decouples the logit order from the adaptation for conformal prediction, allowing C-Adapter to focus on optimizing efficiency. We demonstrate the superiority of this adaptation strategy over others in Figures 5 and 6.

Training objective ConfTr optimizes the efficiency of conformal predictors at a predetermined error rate (e.g., $\alpha = 0.01$), which may result in suboptimal performance when predicting with a different coverage rate. To address this issue, we consider a general criterion for efficiency:

$$\mathbb{E}_{\boldsymbol{x}\sim\mathcal{P}_{\mathcal{X}}}\left[\int_0^1 |\mathcal{C}(\boldsymbol{x};\tau_\alpha,\widetilde{\pi}_{\boldsymbol{w}})|\,\mathrm{d}\alpha\right], \tag{4}$$

which measures the definite integral of efficiency over $\alpha \in (0,1)$. For notation shorthand, we use $\widetilde{\pi}_{\boldsymbol{w}}$ to indicate that the underlying classifier f is equipped with C-Adapter, parameterized by $\boldsymbol{w}$. This objective is analogous to the AUC in classification (Cortes & Mohri, 2003), as AUC reflects the classifier's performance across all possible thresholds, while classification error considers only a single fixed one. However, the objective in Equation (4) cannot be directly computed from a given dataset. To address this issue, we translate it into an equivalent form that can be explicitly calculated.

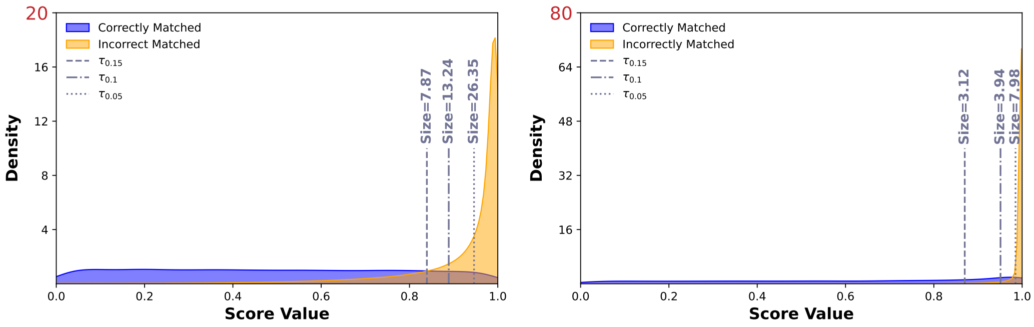

(a) w/o C-Adapter

(b) w/ C-Adapter

Figure 3: **Score distributions of correctly and incorrectly matched data-label pairs:** (a) without C-Adapter, (b) with C-Adapter. We calculate the APS scores on ImageNet using CLIP (Radford et al., 2021). The three gray lines indicate the set sizes with τ_α at $\alpha = 0.15$, 0.1, and 0.05, respectively. Using C-Adapter, the APS scores of incorrect labels tend to be much higher (approaching the maximum 1.0) than those of correct labels. The highly distinguishable scores between correct and incorrect labels translate to more efficient conformal prediction sets at various coverage rates.

From Equation (2), we can infer that we construct the conformal prediction set for $\hat{X} \sim \mathcal{P}_\mathcal{X}$ at α by comparing the non-conformity score $S(\hat{X}, y; \tilde{\pi}_{\boldsymbol{w}})$ with τ_α for each $y \in \mathcal{Y}$. Therefore, it is straightforward to verify that the expected set size at the error rate α over the data distribution $\mathcal{P}_\mathcal{X}$ is determined by the probability of the event $\{\tau_\alpha \geq S(\hat{X}, \hat{Y}; \tilde{\pi}_{\boldsymbol{w}})\}$, where $\hat{X} \sim \mathcal{P}_\mathcal{X}$ and $\hat{Y} \sim \text{Uniform}(\mathcal{Y})$. When extending to any $\alpha \in (0, 1)$, the threshold τ_α can be the non-conformity score of any observation $(X, Y) \sim \mathcal{P}_{\mathcal{X}\mathcal{Y}}$. This prompts us to consider the following probability:

$$\mathbb{P}\left(S(X, Y; \tilde{\pi}_{\boldsymbol{w}}) \geq S(\hat{X}, \hat{Y}; \tilde{\pi}_{\boldsymbol{w}})\right), \text{where } (X, Y) \sim \mathcal{P}_{\mathcal{X}\mathcal{Y}}, \hat{X} \sim \mathcal{P}_\mathcal{X}, \hat{Y} \sim \text{Uniform}(\mathcal{Y}). \tag{5}$$

In particular, this probability quantifies the likelihood that the non-conformity score of a randomly matched data-label pair $(\hat{X}, \hat{Y})$ is not greater than that of a correctly matched pair (X, Y) . This probability approaches zero when the scores of correctly and incorrectly matched data-label pairs are well distinguishable, and approaches $1/2$ when they are not effectively distinguished. In the following, we present a formal analysis demonstrating that minimizing the probability in Equation (5) is equivalent to optimizing the overall efficiency defined in Equation (4).

Proposition 1. *Let $\hat{\pi}$ and $\hat{\pi}'$ be pre-trained classifiers with parameters θ and θ', respectively, and let S be a specific non-conformity score function. We denote $\mathcal{P}_{S_\theta}$ and $\mathcal{P}_{S_{\theta'}}$ as the distributions of $S(X, Y; \hat{\pi})$ and $S(X, Y; \hat{\pi}')$, where $(X, Y) \sim \mathcal{P}_{\mathcal{X}\mathcal{Y}}$. Let F_{S_θ}, and $F_{S_{\theta'}}$ be the CDF corresponding to $\mathcal{P}_{S_\theta}$ and $\mathcal{P}_{S_{\theta'}}$. Given that $\hat{X} \sim \mathcal{P}_\mathcal{X}$ and $\hat{Y}$ follows a uniform distribution over $\mathcal{Y}$, we have*

$$\mathbb{P}\left(S(X, Y; \hat{\pi}) \geq S(\hat{X}, \hat{Y}; \hat{\pi})\right) > \mathbb{P}\left(S(X, Y; \hat{\pi}') \geq S(\hat{X}, \hat{Y}; \hat{\pi}')\right)$$

holds if and only if

$$\mathbb{E}_{X \sim \mathcal{P}_\mathcal{X}}\left[\int_0^1 |\mathcal{C}\left(X; F_{S_\theta}^{-1}(1-\alpha), \hat{\pi}\right)| \, \mathrm{d}\alpha\right] > \mathbb{E}_{X \sim \mathcal{P}_\mathcal{X}}\left[\int_0^1 |\mathcal{C}\left(X; F_{S_{\theta'}}^{-1}(1-\alpha), \hat{\pi}'\right)| \, \mathrm{d}\alpha\right].$$

The proof of Proposition 1 is provided in Appendix E. Here, the inverse CDF calculates the $(1-\alpha)$-th quantile of the score distributions, which determines the threshold τ_α. Then, to optimize overall efficiency in Equation (4), we turn to minimize the following objective, rewritten from Equation (5):

$$\mathcal{L}(\boldsymbol{w}) = \mathbb{E}\left[\mathbb{1}_{\{S(X, Y; \tilde{\pi}_{\boldsymbol{w}}) > S(\hat{X}, \hat{Y}; \tilde{\pi}_{\boldsymbol{w}})\}}\right], \tag{6}$$

where $(X, Y) \sim \mathcal{P}_{\mathcal{X}\mathcal{Y}}$, $\hat{X} \sim \mathcal{P}_\mathcal{X}$, and $\hat{Y} \sim \text{Uniform}(\mathcal{Y})$. Given the non-differentiability of the indicator function, it is common practice to utilize surrogate functions as differentiable approximations (Yan et al., 2003; Yuan et al., 2021). In this work, we apply the sigmoid function with a parameter T as the surrogate, defined as $\sigma_T(x) = 1/\left(1 + \exp\left(-x/T\right)\right)$. For the score function utilized during training, we employ either THR or APS. The differentiable APS is implemented as outlined in

ConfTr (Stutz et al., 2021). Ultimately, the convex relaxation of Equation (6) is given by

$$\widetilde{\mathcal{L}}(\boldsymbol{w}) = \mathbb{E}\left[\sigma_T\left(S(X, Y; \widetilde{\pi}_{\boldsymbol{w}}) - S(\hat{X}, \hat{Y}; \widetilde{\pi}_{\boldsymbol{w}})\right)\right]. \tag{7}$$

By optimizing this objective, the scores of correctly and incorrectly matched data-label pairs become more distinguishable: correctly matched pairs are encouraged to have relatively smaller non-conformity scores compared to incorrectly matched pairs. We visualize this effect in Figure 3. With C-Adapter, the APS scores of incorrect labels become significantly higher than those of correct labels, leading to more efficient prediction sets across varying coverage rates. Moreover, our proposed objective achieves superior average performance compared to the size loss of ConfTr (see Table 2).

Batched optimization In the t-th iteration, we construct an auxiliary batch $\hat{\mathcal{B}}_t$ by creating K data-label pairs for each instance in $\mathcal{B}_t$. Each pair $(\hat{\boldsymbol{x}}, \hat{y})$ in $\hat{\mathcal{B}}_t$ consists of an instance from $\mathcal{B}_t$ and one of the K possible labels $\hat{y} \in \mathcal{Y}$. Subsequently, we update the parameters $\boldsymbol{w}$ of C-Adapter by

$$\boldsymbol{w}^{(t)} \leftarrow \boldsymbol{w}^{(t-1)} - \eta_t \cdot \nabla_{\boldsymbol{w}} \left[\frac{1}{|\mathcal{B}_t| \cdot |\hat{\mathcal{B}}_t|} \sum_{(\boldsymbol{x}, y) \in \mathcal{B}_t} \sum_{(\hat{\boldsymbol{x}}, \hat{y}) \in \hat{\mathcal{B}}_t} \sigma_T\left(S\left(\boldsymbol{x}, y; \widetilde{\pi}_{\boldsymbol{w}}\right) - S\left(\hat{\boldsymbol{x}}, \hat{y}; \widetilde{\pi}_{\boldsymbol{w}}\right)\right)\right]. \tag{8}$$

The optimization incurs low computational costs, as we only update the parameters of the linear layers in C-Adapter. In practical applications, we tune the parameters of C-Adapter using the training set for the trained classifier f. Our method can also be implemented with a hold-out set, which is explicitly validated in Figure 8. Noticeably, our method offers several compelling advantages:

- **Flexible:** C-Adapter can enhance the efficiency of conformal predictors across different non-conformity score functions, not limited to the one employed during its tuning (see Table 1 and Table 5). By default, we tune C-Adapter using THR.
- **Easy to use:** C-Adapter requires minimal hyperparameter tuning and performs well with any sufficiently small T (see Figure 7). Moreover, our method shows high computational efficiency and a rapid convergence rate (refer to the convergence analysis in Appendix F).
- **Model-agnostic:** C-Adapter requires access only to the model outputs and integrates effortlessly with any classifier. Our method can effectively adapt trained classifiers for efficient prediction sets, regardless of the network architecture or pre-training strategy.

4 EXPERIMENTS

4.1 EXPERIMENTAL SETUP

Dataset We evaluate our approach using three benchmarks of image classification: CIFAR-100 (Krizhevsky et al., 2009), ImageNet (Deng et al., 2009), and ImageNet-V2 (Recht et al., 2019). For CIFAR-100 and ImageNet-V2, we randomly split the test sets into calibration and test subsets, each containing 5,000 samples. For ImageNet, we partition the 50,000-sample test dataset into a calibration subset of 30,000 samples and a test subset of 20,000 samples.

Models For our evaluations, we utilize four well-established deep image classifiers: ResNet101 (RN101) (He et al., 2016), two variants of DenseNet (DN121 and DN161) (Huang et al., 2017), and ResNeXt50 (RNX50) (Xie et al., 2017). Additionally, we employ the Vision-Language Model CLIP (Radford et al., 2021), which is based on a Vision Transformer architecture (ViT-B/16) (Dosovitskiy et al., 2020). For ImageNet, we leverage pre-trained deep image classifiers from TorchVision (Paszke et al., 2019), whereas for CIFAR-100, we train the classifiers from scratch using the entire training set. For CLIP, we rely on its inherent zero-shot capabilities to perform classification tasks.

Training details C-Adapter is tuned for 240 *iterations* using Adam (Kingma & Ba, 2014), with a batch size of 256 and a learning rate of 0.1. The parameter T is set to 0.0001 by default. We partition the calibration set into a validation subset and a calibration subset in an 20:80 ratio, with the validation set used for early stopping. When a validation set is not necessary, the entire calibration set is employed for calibration, ensuring all methods have access to the same dataset. To ensure the reliability of our results, each experiment is repeated 10 times, and the average result is reported. All experiments are conducted on an NVIDIA GeForce RTX 4090 using PyTorch (Paszke et al., 2019).

Table 1: **Performance of C-Adapter on common benchmarks.** ↓ indicates that a smaller value is better. Results in **bold** indicate superior performance. C-Adapter is tuned using THR.

Score	Model	w/o C-Adapter \ w/ C-Adapter							
		ImageNet				CIFAR-100			
		$\alpha = 0.05$		$\alpha = 0.1$		$\alpha = 0.05$		$\alpha = 0.1$	
		Coverage	Size (↓)	Coverage	Size (↓)	Cover	Size (↓)	Coverage	Size (↓)
THR	RN101	0.95 \ 0.95	4.03 \ **3.82**	0.90 \ 0.90	1.91 \ **1.89**	0.95 \ 0.95	3.64 \ **3.17**	0.90 \ 0.90	1.87 \ **1.76**
	DN121	0.95 \ 0.95	5.66 \ **5.35**	0.90 \ 0.90	2.42 \ **2.34**	0.95 \ 0.95	3.27 \ **3.00**	0.90 \ 0.90	1.72 \ **1.70**
	DN161	0.95 \ 0.95	4.03 \ **3.69**	0.90 \ 0.90	1.89 \ **1.82**	0.95 \ 0.95	2.91 \ **2.75**	0.90 \ 0.90	1.72 \ **1.69**
	RNX50	0.95 \ 0.95	4.26 \ **3.87**	0.90 \ 0.90	1.87 \ **1.85**	0.95 \ 0.95	3.41 \ **3.09**	0.90 \ 0.90	1.78 \ **1.76**
	CLIP	0.95 \ 0.95	6.88 \ **6.71**	0.90 \ 0.90	3.33 \ **3.25**	0.95 \ 0.95	9.71 \ **8.25**	0.90 \ 0.90	4.78 \ **4.36**
	Average	0.95 \ 0.95	4.97 \ **4.69**	0.90 \ 0.90	2.29 \ **2.23**	0.95 \ 0.95	4.59 \ **4.05**	0.90 \ 0.90	2.37 \ **2.25**
APS	RN101	0.95 \ 0.95	14.73 \ **3.98**	0.90 \ 0.90	7.23 \ **2.30**	0.95 \ 0.95	7.60 \ **3.19**	0.90 \ 0.90	3.95 \ **1.86**
	DN121	0.95 \ 0.95	20.00 \ **5.73**	0.90 \ 0.90	9.21 \ **2.86**	0.95 \ 0.95	10.20 \ **3.08**	0.90 \ 0.90	5.39 \ **1.85**
	DN161	0.95 \ 0.95	16.43 \ **4.23**	0.90 \ 0.90	6.82 \ **2.33**	0.95 \ 0.95	9.90 \ **2.86**	0.90 \ 0.90	5.42 \ **1.80**
	RNX50	0.95 \ 0.95	21.54 \ **4.26**	0.90 \ 0.90	8.92 \ **2.32**	0.95 \ 0.95	9.95 \ **3.26**	0.90 \ 0.90	5.14 \ **1.91**
	CLIP	0.95 \ 0.95	26.35 \ **7.98**	0.90 \ 0.90	13.24 \ **3.94**	0.95 \ 0.95	16.13 \ **13.50**	0.90 \ 0.90	10.18 \ **8.70**
	Average	0.95 \ 0.95	19.81 \ **5.24**	0.90 \ 0.90	9.08 \ **2.75**	0.95 \ 0.95	10.76 \ **5.18**	0.90 \ 0.90	6.01 \ **3.22**
RAPS	RN101	0.95 \ 0.95	7.13 \ **3.75**	0.90 \ 0.90	4.60 \ **2.25**	0.95 \ 0.95	5.16 \ **4.43**	0.90 \ 0.90	3.25 \ **1.81**
	DN121	0.95 \ 0.95	10.28 \ **6.53**	0.90 \ 0.90	6.57 \ **2.80**	0.95 \ 0.95	7.19 \ **3.74**	0.90 \ 0.90	4.50 \ **1.80**
	DN161	0.95 \ 0.95	7.31 \ **4.10**	0.90 \ 0.90	4.63 \ **2.27**	0.95 \ 0.95	7.10 \ **3.15**	0.90 \ 0.90	4.59 \ **1.79**
	RNX50	0.95 \ 0.95	7.87 \ **4.11**	0.90 \ 0.90	5.20 \ **2.26**	0.95 \ 0.95	7.20 \ **3.94**	0.90 \ 0.90	4.47 \ **1.89**
	CLIP	0.95 \ 0.95	15.14 \ **7.82**	0.90 \ 0.90	9.25 \ **3.49**	0.95 \ 0.95	14.52 \ **11.19**	0.90 \ 0.90	9.41 \ **7.62**
	Average	0.95 \ 0.95	9.55 \ **5.26**	0.90 \ 0.90	6.05 \ **2.61**	0.95 \ 0.95	8.24 \ **5.45**	0.90 \ 0.90	5.24 \ **2.98**

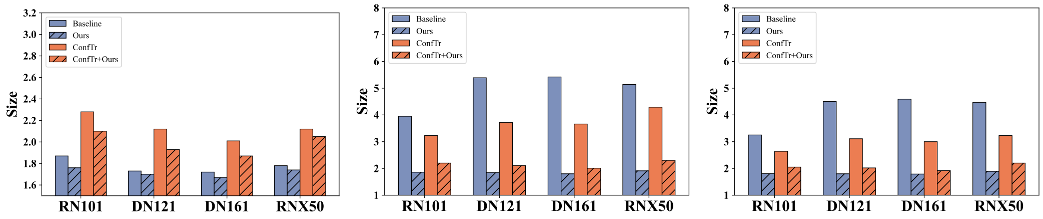

(a) THR (b) APS (c) RAPS

Figure 4: **Comparison of C-Adapter and ConfTr,** using (a) THR, (b) APS, and (c) RAPS at $\alpha = 0.1$ on CIFAR-100. "ConfTr + Ours" refers to applying C-Adapter to models that have been fine-tuned using ConfTr. The results demonstrate that C-Adapter outperforms ConfTr.

Evaluation metrics The primary metrics for evaluating prediction sets are: (1) efficiency (Size) and (2) marginal coverage rate (Coverage). Moreover, we assess conditional coverage using (1) class-conditional coverage gap (CovGap) (Ding et al., 2024) and (2) size-stratified coverage violation (SSCV) (Angelopoulos et al., 2020). We detail these metrics in Appendix G.

4.2 RESULTS

C-Adapter improves the efficiency of conformal predictors. In Table 1, we present the performance of THR, APS, and RAPS with C-Adapter on ImageNet and CIFAR-100. A salient observation is that our method drastically improves the efficiency of conformal predictors with the desired coverage rate. For example, C-Adapter reduces the size of APS from 16.43 to 4.23 on ImageNet using DN161 with $\alpha = 0.05$. Notably, the improvements remain substantial when there is a mismatch between the score functions used during adapter tuning (THR) and those employed in conformal prediction (APS and RAPS). When C-Adapter is tuned with APS, similar enhancements are observed with both THR and RAPS, as detailed in Appendix I. This highlights the flexibility of our method. Overall, empirical results show that C-Adapter can enhance the efficiency of conformal predictors across various score functions, regardless of model architectures and pre-training strategies.

C-Adapter outperforms ConfTr. ConfTr (Stutz et al., 2021) can be employed as a fine-tuning method to adapt classifiers for conformal prediction. Initially, the classifier is trained with cross-entropy loss, and then only the fully connected layer is tuned using the objective in Equation (3). We

Table 2: **Comparison of C-Adapter with different loss functions,** on ImageNet with DN121. Baseline represents the scenario without C-Adapter. Since each entry achieves the desired coverage, only **Size** is presented. Our loss achieves superior average performance compared to the size loss.

	THR							**APS**						
α	**0.06**	**0.05**	**0.04**	**0.03**	**0.02**	**0.01**	**Average**	**0.06**	**0.05**	**0.04**	**0.03**	**0.02**	**0.01**	**Average**
Baseline	4.35	5.66	7.26	10.46	15.91	33.84	12.91	15.94	20.00	24.42	32.62	48.13	91.49	38.77
size loss	**4.26**	**5.33**	7.04	9.93	17.44	43.16	14.53	4.48	**5.71**	7.39	10.82	18.82	42.63	14.98
Ours	4.27	5.35	**6.94**	**9.75**	**15.01**	**30.31**	**11.94**	**4.44**	5.73	**7.37**	**10.70**	**17.30**	**36.24**	**13.63**

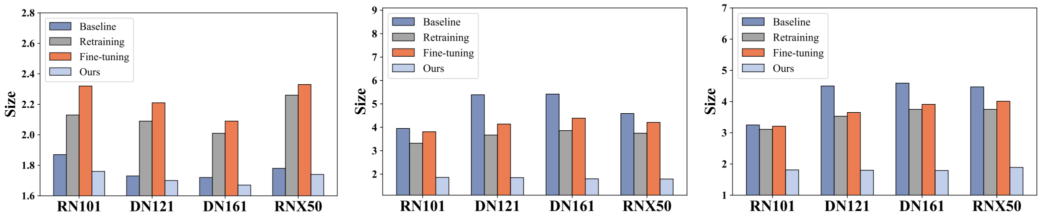

(a) THR

(b) APS

(c) RAPS

Figure 5: **Comparison of different adaptation strategies,** using (a) THR, (b) APS, and (c) RAPS at $\alpha = 0.1$. The experiment is conducted on CIFAR-100. *Retraining* refers to training the classifier from scratch with our proposed loss function, while *Fine-tuning* indicates tuning only the fully connected layer with our loss. C-Adapter outperforms the other two adaptation strategies.

compare this approach with ours on CIFAR-100. For ConfTr, we set the learning rate to 0.001 with a batch size of 256. A higher learning rate significantly decreases classification accuracy, leading to a dramatic decline in efficiency. The parameters T and λ are tuned from the sets $\{0.01, 0.1, 0.5, 1\}$ and $\{0.005, 0.01, 0.05, 0.1, 0.2\}$, respectively. During training, we utilize THRLP (Stutz et al., 2021) for ConfTr, setting α to 0.01. For evaluation, we employ THR, APS, and RAPS with $\alpha = 0.1$.

Our results in Figure 4 illustrate the superior performance of our approach. For APS and RAPS, both C-Adapter and ConfTr improve the efficiency of conformal predictors, with C-Adapter demonstrating superior performance. Furthermore, C-Adapter enhances the efficiency of THR, whereas ConfTr does not. Additionally, we apply C-Adapter to models that have already been fine-tuned using ConfTr. The results indicate that our approach can further improve the performance of ConfTr. Notably, Baseline+C-Adapter outperforms ConfTr+C-Adapter, suggesting that the accuracy decline associated with ConfTr limits the efficiency of conformal predictors. Overall, empirical results demonstrate that C-Adapter not only surpasses ConfTr but can also enhance its performance.

Ablation study on the adaptation strategy To further demonstrate the significance of this adapter-based tuning method, this ablation compares our approach with two alternative strategies: (1) *Retraining*, which involves training the classifier from scratch with our proposed loss function, and (2) *Fine-tuning*, where the classifier is initially trained with cross-entropy loss and subsequently fine-tuned only on the fully connected layer with our loss. The second strategy is analogous to ConfTr, but it employs a different loss function. In our approach, we first train the classifier using cross-entropy loss and then adapt it for conformal prediction with C-Adapter. This ablation employs a consistent loss function to ensure a fair comparison among different adaptation strategies. We provide the detailed experimental setup for the competing methods in Appendix H.2.

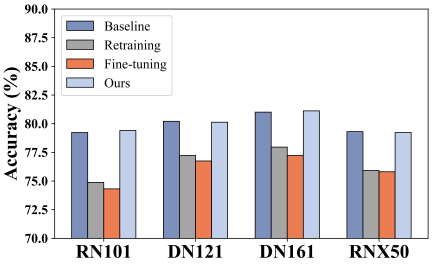

Figure 6: **Accuracy of various adaptation strategies,** on CIFAR-100. Both *Retraining* and *Fine-tuning* result in 3-5% lower accuracy compared to the baseline.

As demonstrated in Figure 6, both *Retraining* and *Fine-tuning* result in 3-5% lower accuracy compared to the baseline. Our results in Figure 5 empirically demonstrate that this decline in accuracy limits overall efficiency: while all three adaptation strategies can enhance the efficiency of APS and RAPS, our method significantly outperforms the others. The negative impact of decreased accu-

Table 3: **Experimental results on conditional coverage.** This experiment is conducted on ImageNet. ↓ indicates that smaller values are preferable. Since each entry achieves the desired coverage, **Coverage** is omitted. C-Adapter consistently reduces Size, SSCV, and CovGap in most cases.

		Size ↓ / SSCV ↓ / CovGap ↓					
		RN101	**DN121**	**DN161**	**RNX50**	**CLIP**	**Average**
$\alpha = 0.05$	APS	14.73 / 3.07 / 4.30	20.00 / 2.48 / 4.39	16.43 / 3.16 / 4.49	21.54 / 5.09 / 4.50	26.35 / 3.25 / 4.94	19.81 / 3.41 / 4.52
	+Ours	**11.00 / 2.05 / 4.27**	**13.39 / 1.79 / 4.37**	**10.87 / 2.69 / 4.38**	**12.98 / 2.93 / 4.38**	**17.21 / 2.23 / 4.90**	**13.09 / 2.34 / 4.46**
	RAPS	7.13 / 2.35 / 4.37	10.28 / 2.95 / **4.50**	7.31 / 3.17 / 4.36	7.87 / 3.83 / 4.60	15.14 / 1.78 / 5.07	9.55 / 2.82 / 4.58
	+Ours	**6.98 / 1.99 / 4.27**	**8.87 / 1.88** / 4.61	**6.48 / 2.34 / 4.31**	**6.79 / 2.67 / 4.52**	**12.55 / 1.71 / 4.97**	**8.41 / 2.12 / 4.54**
$\alpha = 0.1$	APS	7.23 / 5.97 / 6.03	9.21 / 5.76 / **5.69**	6.82 / 5.76 / **5.70**	8.92 / 7.26 / 6.09	13.24 / 6.87 / 7.47	9.08 / 6.32 / 6.20
	+Ours	**5.75 / 5.85 / 5.93**	**6.56 / 1.89** / 5.75	**5.21 / 1.91** / 5.77	**6.48 / 4.36 / 6.05**	**9.38 / 3.51 / 7.44**	**6.68 / 3.78 / 6.19**
	RAPS	4.60 / 4.56 / 6.15	6.57 / 2.98 / **5.71**	4.63 / 3.93 / **6.12**	5.20 / 2.87 / 6.16	9.25 / 3.44 / 7.51	6.05 / 3.56 / 6.33
	+Ours	**4.45 / 4.12 / 6.02**	**5.89 / 2.87** / 5.78	**4.31 / 3.73** / 6.18	**4.75 / 2.67 / 6.13**	**7.82 / 2.40** / 7.51	**5.44 / 3.16 / 6.32**

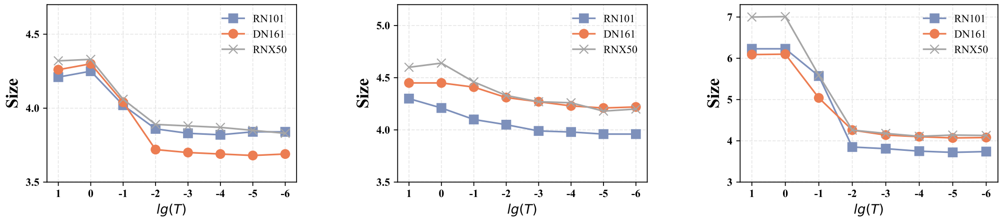

(a) THR (b) APS (c) RAPS

Figure 7: Effect of T on the efficiency of prediction sets with (a) THR, (b) APS, and (c) RAPS.

racy is particularly evident in THR, where only our method achieves an improvement in efficiency. Overall, this ablation study further highlights the superiority of our adaptation strategy.

Ablation study on the loss function The size loss from ConfTr can also be utilized to tune our conformal adapter. We conduct an ablation study on ImageNet using DN121, comparing C-Adapter with size loss against our proposed loss function. For the size loss, we maintain a consistent experimental setup and tune the parameter T within the range $\{0.0001, 0.001, 0.01, 0.1\}$, while setting the error rate α to 0.01 during training. For evaluation, we use THR and APS at various coverage rates.

Our results in Table 2 indicate that C-Adapter effectively integrates with size loss, enhancing the efficiency of conformal predictors regardless of the employed score function. However, our proposed loss function achieves superior average performance. Notably, size loss performs poorly at small error rates α; it exhibits inferior performance compared to the baseline when utilizing THR at $\alpha = 0.01$ and $\alpha = 0.02$, while our method consistently outperforms the baseline. Overall, this analysis highlights the flexibility of C-Adapter and the efficacy of our proposed loss function.

C-Adapter can reduce conditional coverage violations. As shown in Table 1, C-Adapter can enhance the efficiency of THR, APS, and RAPS. However, unlike THR, which seeks optimal efficiency with limited conditional coverage, APS is designed to improve the conditional coverage of prediction sets. RAPS also aims to enhance conditional coverage while simultaneously boosting efficiency. In this study, we further demonstrate that C-Adapter can enhance the conditional coverage of APS and RAPS. All experimental setups remain consistent, except that training concludes at the iteration corresponding to the *optimal SSCV* instead of Size on the validation set.

As detailed in Table 3, C-Adapter consistently reduces Size, SSCV, and CovGap in most cases under this setting. Notably, the reduction in Size is less substantial compared to the results in Table 1. *Thus, users can adopt an early stopping strategy that best aligns with their specific needs for efficiency and conditional coverage.* Overall, this experiment validates that C-Adapter can enhance the conditional coverage of APS and RAPS while simultaneously improving their efficiency.

How does the parameter T affect the performance of C-Adapter? In Figure 7, we ablate how the parameter T introduced by the surrogate function affects the efficiency of conformal predictors, using THR, APS, and RAPS. We set the error rate α to 0.05. As demonstrated in this figure, C-Adapter with a sufficiently small T (below 0.01) stably enhances the efficiency of conformal predictors. This is because the sigmoid function in Equation (7) approximates the indicator function when T is small. For simplicity, we set $T = 10^{-4}$ throughout the experiments.

Table 4: **The robustness of C-Adapter to distribution shift.** C-Adapter is tuned using ImageNet and tested on ImageNet-V2. Since each entry achieves the desired coverage, only **Size** is presented.

Model	**w/o C-Adapter \ w/ C-Adapter**					
	THR		**APS**		**RAPS**	
	α =0.1	α =0.2	α =0.1	α =0.2	α =0.1	α =0.2
RN101	6.03 \ **5.43**	2.11 \ **2.01**	19.65 \ **5.59**	7.17 \ **2.57**	10.90 \ **7.01**	5.67 \ **2.29**
DN121	8.01 \ **7.70**	2.60 \ **2.52**	24.73 \ **8.14**	9.13 \ **3.21**	14.31 \ **10.38**	7.20 \ **3.01**
DN161	5.41 \ **4.72**	2.06 \ **1.91**	19.32 \ **5.21**	6.31 \ **2.52**	10.27 \ **5.98**	5.18 \ **2.18**
RNX50	6.80 \ **5.78**	2.07 \ **2.05**	26.27 \ **6.11**	8.58 \ **2.63**	11.43 \ **7.83**	6.14 \ **2.38**
CLIP	5.66 \ **5.59**	2.31 \ **2.29**	20.73 \ **14.88**	8.21 \ **6.60**	10.60 \ **8.67**	6.35 \ **6.10**
Average	6.38 \ **5.84**	2.23 \ **2.16**	22.14 \ **7.99**	7.88 \ **3.51**	11.50 \ **7.97**	6.11 \ **3.19**

C-Adapter shows robustness to distribution shifts. We investigate the robustness of C-Adapter to distribution shifts. Specifically, we tune C-Adapter using the training set of ImageNet and split ImageNet-V2 into two equal-sized calibration and test sets. Notably, the shifts happen between the training set and calibration/test sets. Thus, coverage will not be affected, as the calibration and test sets remain exchangeable. We examine the performance of C-Adapter on APS, THR, and RAPS at $\alpha = 0.1$ and $\alpha = 0.2$. As demonstrated in Table 4, C-Adapter consistently reduces Size across various base classifiers on ImageNet-V2, regardless of the score function or the predefined error rate α. For example, when evaluated on DN161 with $\alpha = 0.1$, C-Adapter reduces the Size of APS from 19.32 to 5.21. The results highlight the robustness of C-Adapter to distribution shifts. We further investigate the robustness of C-Adapter under different kinds of data shifts in Appendix I.

Does C-Adapter perform better with a hold-out set for training? In the original setup, we train C-Adapter using the training set for the classifier f. In this ablation, we investigate whether C-Adapter benefits from using a hold-out set for training. Specifically, we randomly divide the ImageNet test set into 10,000 samples for training, 20,000 for calibration and validation, and 20,000 for testing. C-Adapter is tuned for 2 epochs using the 10,000-sample training set with Adam, a batch size of 256, and a learning rate of 0.1, while the parameter T is set to 0.0001. For evaluation, we utilize THR and APS with an error rate of 0.05.

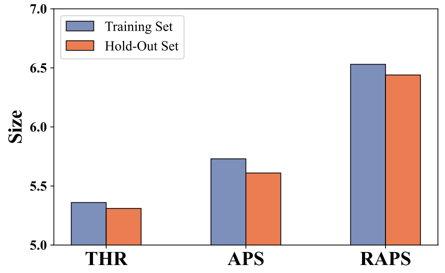

Figure 8: Comparison of tuning C-Adapter using a hold-out set vs. the original training set on ImageNet with DN121.

Our results in Figure 8 indicate that C-Adapter demonstrates improved performance when utilizing a hold-out set for training, irrespective of the score function employed. However, this improvement is not statistically significant. We conclude that using the original training set is sufficient for adapting the classifier to achieve more efficient prediction sets, which also enables more efficient data utilization.

5 CONCLUSION

In this paper, we introduce C-Adapter, an adapter-based tuning method to enhance the efficiency of conformal predictors. Our key idea is to adapt the trained classifiers for conformal prediction while preserving the ranking of labels in the output logits, thereby maintaining the top-k accuracy of the classifiers. To achieve this, we implement the adapter as a class of intra order-preserving functions. For the optimization of C-Adapter, we propose a loss function that enhances the discriminability of non-conformity scores between correctly and randomly matched data-label pairs. Extensive experiments demonstrate that C-Adapter effectively adapts various classifiers for efficient prediction sets and enhances the conformal training method. Our method is user-friendly, as it does not require heavy tuning of hyperparameters and computationally efficient. We hope the insights from this work will inspire future research to explore more effective adaptation strategies for conformal prediction.

Limitation Although our adaptation strategy demonstrates promise, we focus solely on using it to optimize the efficiency of conformal predictors. Developing targeted loss functions to adapt deep classifiers for other aspects of conformal prediction (e.g., conditional coverage or robustness) is not explored in this work and offers an interesting direction for future research.

REFERENCES

Anastasios N Angelopoulos and Stephen Bates. A gentle introduction to conformal prediction and distribution-free uncertainty quantification. *arXiv preprint arXiv:2107.07511*, 2021.

Anastasios Nikolas Angelopoulos, Stephen Bates, Michael Jordan, and Jitendra Malik. Uncertainty sets for image classifiers using conformal prediction. In *International Conference on Learning Representations*, 2020.

Vineeth Balasubramanian, Shen-Shyang Ho, and Vladimir Vovk. *Conformal prediction for reliable machine learning: theory, adaptations and applications*. Newnes, 2014.

Anthony Bellotti. Optimized conformal classification using gradient descent approximation. *arXiv preprint arXiv:2105.11255*, 2021.

Mathieu Blondel, Olivier Teboul, Quentin Berthet, and Josip Djolonga. Fast differentiable sorting and ranking. In *International Conference on Machine Learning*, pp. 950–959. PMLR, 2020.

John J Cherian, Isaac Gibbs, and Emmanuel J Candès. Large language model validity via enhanced conformal prediction methods. *arXiv preprint arXiv:2406.09714*, 2024.

Alvaro HC Correia, Fabio Valerio Massoli, Christos Louizos, and Arash Behboodi. An information theoretic perspective on conformal prediction. *arXiv preprint arXiv:2405.02140*, 2024.

Corinna Cortes and Mehryar Mohri. AUC optimization vs. error rate minimization. *Advances in neural information processing systems*, 16, 2003.

Marco Cuturi, Olivier Teboul, and Jean-Philippe Vert. Differentiable ranking and sorting using optimal transport. *Advances in neural information processing systems*, 32, 2019.

Jia Deng, Wei Dong, Richard Socher, Li-Jia Li, Kai Li, and Li Fei-Fei. Imagenet: A large-scale hierarchical image database. In *2009 IEEE conference on computer vision and pattern recognition*, pp. 248–255. Ieee, 2009.

Tiffany Ding, Anastasios Angelopoulos, Stephen Bates, Michael Jordan, and Ryan J Tibshirani. Class-conditional conformal prediction with many classes. *Advances in Neural Information Processing Systems*, 36, 2024.

Alexey Dosovitskiy, Lucas Beyer, Alexander Kolesnikov, Dirk Weissenborn, Xiaohua Zhai, Thomas Unterthiner, Mostafa Dehghani, Matthias Minderer, Georg Heigold, Sylvain Gelly, et al. An image is worth 16x16 words: Transformers for image recognition at scale. *arXiv preprint arXiv:2010.11929*, 2020.

Bat-Sheva Einbinder, Yaniv Romano, Matteo Sesia, and Yanfei Zhou. Training uncertainty-aware classifiers with conformalized deep learning. *Advances in Neural Information Processing Systems*, 35:22380–22395, 2022.

Chuan Guo, Geoff Pleiss, Yu Sun, and Kilian Q Weinberger. On calibration of modern neural networks. In *International conference on machine learning*, pp. 1321–1330. PMLR, 2017.

Kaiming He, Xiangyu Zhang, Shaoqing Ren, and Jian Sun. Deep residual learning for image recognition. In *Proceedings of the IEEE conference on computer vision and pattern recognition*, pp. 770–778, 2016.

Dan Hendrycks, Steven Basart, Norman Mu, Saurav Kadavath, Frank Wang, Evan Dorundo, Rahul Desai, Tyler Zhu, Samyak Parajuli, Mike Guo, et al. The many faces of robustness: A critical analysis of out-of-distribution generalization. In *Proceedings of the IEEE/CVF international conference on computer vision*, pp. 8340–8349, 2021a.

Dan Hendrycks, Kevin Zhao, Steven Basart, Jacob Steinhardt, and Dawn Song. Natural adversarial examples. In *Proceedings of the IEEE/CVF conference on computer vision and pattern recognition*, pp. 15262–15271, 2021b.

Eliahu Horwitz and Yedid Hoshen. Conffusion: Confidence intervals for diffusion models. *arXiv preprint arXiv:2211.09795*, 2022.

Neil Houlsby, Andrei Giurgiu, Stanislaw Jastrzebski, Bruna Morrone, Quentin De Laroussilhe, Andrea Gesmundo, Mona Attariyan, and Sylvain Gelly. Parameter-efficient transfer learning for nlp. In *International conference on machine learning*, pp. 2790–2799. PMLR, 2019.

Edward J Hu, Yelong Shen, Phillip Wallis, Zeyuan Allen-Zhu, Yuanzhi Li, Shean Wang, Lu Wang, and Weizhu Chen. Lora: Low-rank adaptation of large language models. *arXiv preprint arXiv:2106.09685*, 2021.

Gao Huang, Zhuang Liu, Laurens Van Der Maaten, and Kilian Q Weinberger. Densely connected convolutional networks. In *Proceedings of the IEEE conference on computer vision and pattern recognition*, pp. 4700–4708, 2017.

Jianguo Huang, Huajun Xi, Linjun Zhang, Huaxiu Yao, Yue Qiu, and Hongxin Wei. Conformal prediction for deep classifier via label ranking. In *International Conference on Machine Learning (ICML)*, 2024a.

Kexin Huang, Ying Jin, Emmanuel Candes, and Jure Leskovec. Uncertainty quantification over graph with conformalized graph neural networks. *Advances in Neural Information Processing Systems*, 36, 2024b.

Diederik P Kingma and Jimmy Ba. Adam: A method for stochastic optimization. *arXiv preprint arXiv:1412.6980*, 2014.

Alex Krizhevsky, Geoffrey Hinton, et al. Learning multiple layers of features from tiny images. 2009.

Jens Lehmann, Robert Isele, Max Jakob, Anja Jentzsch, Dimitris Kontokostas, Pablo N Mendes, Sebastian Hellmann, Mohamed Morsey, Patrick Van Kleef, Sören Auer, et al. Dbpedia–a large-scale, multilingual knowledge base extracted from wikipedia. *Semantic web*, 6(2):167–195, 2015.

Lars Lindemann, Yiqi Zhao, Xinyi Yu, George J Pappas, and Jyotirmoy V Deshmukh. Formal verification and control with conformal prediction. *arXiv preprint arXiv:2409.00536*, 2024.

Kangdao Liu, Tianhao Sun, Hao Zeng, Yongshan Zhang, Chi-Man Pun, and Chi-Man Vong. Spatial-aware conformal prediction for trustworthy hyperspectral image classification. *arXiv preprint arXiv:2409.01236*, 2024.

Rui Luo and Zhixin Zhou. Trustworthy classification through rank-based conformal prediction sets. *arXiv preprint arXiv:2407.04407*, 2024.

Adam Paszke, Sam Gross, Francisco Massa, Adam Lerer, James Bradbury, Gregory Chanan, Trevor Killeen, Zeming Lin, Natalia Gimelshein, Luca Antiga, et al. Pytorch: An imperative style, high-performance deep learning library. *Advances in neural information processing systems*, 32, 2019.

Alec Radford, Jong Wook Kim, Chris Hallacy, Aditya Ramesh, Gabriel Goh, Sandhini Agarwal, Girish Sastry, Amanda Askell, Pamela Mishkin, Jack Clark, et al. Learning transferable visual models from natural language supervision. In *International conference on machine learning*, pp. 8748–8763. PMLR, 2021.

Amir Rahimi, Amirreza Shaban, Ching-An Cheng, Richard Hartley, and Byron Boots. Intra order-preserving functions for calibration of multi-class neural networks. *Advances in Neural Information Processing Systems*, 33:13456–13467, 2020.

Sylvestre-Alvise Rebuffi, Hakan Bilen, and Andrea Vedaldi. Learning multiple visual domains with residual adapters. *Advances in neural information processing systems*, 30, 2017.

Benjamin Recht, Rebecca Roelofs, Ludwig Schmidt, and Vaishaal Shankar. Do imagenet classifiers generalize to imagenet? In *International conference on machine learning*, pp. 5389–5400. PMLR, 2019.

Yaniv Romano, Evan Patterson, and Emmanuel Candes. Conformalized quantile regression. *Advances in neural information processing systems*, 32, 2019.

Yaniv Romano, Matteo Sesia, and Emmanuel Candes. Classification with valid and adaptive coverage. *Advances in Neural Information Processing Systems*, 33:3581–3591, 2020.

Mauricio Sadinle, Jing Lei, and Larry Wasserman. Least ambiguous set-valued classifiers with bounded error levels. *Journal of the American Statistical Association*, 114(525):223–234, 2019.

Glenn Shafer and Vladimir Vovk. A tutorial on conformal prediction. *Journal of Machine Learning Research*, 9(3), 2008.

Asa Cooper Stickland and Iain Murray. Bert and pals: Projected attention layers for efficient adaptation in multi-task learning. In *International Conference on Machine Learning*, pp. 5986–5995. PMLR, 2019.

David Stutz, Krishnamurthy Dj Dvijotham, Ali Taylan Cemgil, and Arnaud Doucet. Learning optimal conformal classifiers. In *International Conference on Learning Representations*, 2021.

Jiayuan Su, Jing Luo, Hongwei Wang, and Lu Cheng. Api is enough: Conformal prediction for large language models without logit-access. *arXiv preprint arXiv:2403.01216*, 2024.

Yi-Lin Sung, Jaemin Cho, and Mohit Bansal. Vl-adapter: Parameter-efficient transfer learning for vision-and-language tasks. In *Proceedings of the IEEE/CVF conference on computer vision and pattern recognition*, pp. 5227–5237, 2022.

Hugo Touvron, Thibaut Lavril, Gautier Izacard, Xavier Martinet, Marie-Anne Lachaux, Timothée Lacroix, Baptiste Rozière, Naman Goyal, Eric Hambro, Faisal Azhar, et al. Llama: Open and efficient foundation language models. *arXiv preprint arXiv:2302.13971*, 2023.

Vladimir Vovk. Conditional validity of inductive conformal predictors. In *Proceedings of the Asian Conference on Machine Learning*, pp. 475–490. PMLR, November 2012. `https://proceedings.mlr.press/v25/vovk12.html`.

Vladimir Vovk, Alexander Gammerman, and Glenn Shafer. *Algorithmic learning in a random world*, volume 29. Springer, 2005.

Jun Wang, Jiaming Tong, Kaiyuan Tan, Yevgeniy Vorobeychik, and Yiannis Kantaros. Conformal temporal logic planning using large language models: Knowing when to do what and when to ask for help. *arXiv preprint arXiv:2309.10092*, 2023.

John H Williamson. Differentiable parallel approximate sorting networks, 2020.

Saining Xie, Ross Girshick, Piotr Dollár, Zhuowen Tu, and Kaiming He. Aggregated residual transformations for deep neural networks. In *Proceedings of the IEEE conference on computer vision and pattern recognition*, pp. 1492–1500, 2017.

Lian Yan, Robert H Dodier, Michael Mozer, and Richard H Wolniewicz. Optimizing classifier performance via an approximation to the wilcoxon-mann-whitney statistic. In *Proceedings of the 20th international conference on machine learning (icml-03)*, pp. 848–855, 2003.

Zhuoning Yuan, Yan Yan, Milan Sonka, and Tianbao Yang. Large-scale robust deep auc maximization: A new surrogate loss and empirical studies on medical image classification. In *Proceedings of the IEEE/CVF International Conference on Computer Vision*, pp. 3040–3049, 2021.

Soroush H Zargarbashi, Simone Antonelli, and Aleksandar Bojchevski. Conformal prediction sets for graph neural networks. In *International Conference on Machine Learning*, pp. 12292–12318. PMLR, 2023.

Qingru Zhang, Minshuo Chen, Alexander Bukharin, Nikos Karampatziakis, Pengcheng He, Yu Cheng, Weizhu Chen, and Tuo Zhao. Adalora: Adaptive budget allocation for parameter-efficient fine-tuning. *arXiv preprint arXiv:2303.10512*, 2023.

A RELATED WORK

Conformal prediction has found diverse applications across various domains, including classification (Sadinle et al., 2019), regression (Romano et al., 2019), and more specialized areas such as large language models (Su et al., 2024; Cherian et al., 2024), graph neural networks (Zargarbashi et al., 2023), image generative models (Horwitz & Hoshen, 2022), hyperspectral imaging (Liu et al., 2024), robotic control (Wang et al., 2023), and autonomous systems (Lindemann et al., 2024). In this work, we focus on the split conformal prediction framework (Vovk et al., 2005; Angelopoulos & Bates, 2021), where the training and calibration sets are disjoint. Despite significant progress in developing score functions, such as THR (Sadinle et al., 2019), APS (Romano et al., 2020), RAPS (Angelopoulos et al., 2020), SAPS (Huang et al., 2024a), and RANK (Luo & Zhou, 2024), conformal prediction is typically applied as a post-hoc process for trained classifiers. This separate processing can lead to suboptimal efficiency of conformal predictors.

Adapting deep classifiers for conformal prediction To address the aforementioned issue, several works propose training (fine-tuning) time regularizations to improve the performance of conformal predictors (Stutz et al., 2021; Einbinder et al., 2022; Correia et al., 2024; Huang et al., 2024b). The uncertainty-aware conformal loss function (Einbinder et al., 2022) optimizes the performance of conformal predictors by encouraging the non-conformity scores to follow a uniform distribution, specifically focusing on optimizing APS. To optimize the classifier for maximum predictive efficiency, ConfTr (Stutz et al., 2021) modifies the training objective by introducing a regularization term that minimizes the average set size at a specific error rate. However, this term can negatively impact accuracy by making it challenging to converge to an optimal solution, thereby limiting the overall efficiency of the conformal predictor. Similar works (Huang et al., 2024b; Correia et al., 2024) adopt the ConfTr framework to enhance the efficiency of conformal predictors, yet they still encounter the limitations of ConfTr. Motivated by this, we propose C-Adapter, which enables the efficient adaptation of trained classifiers for conformal prediction without sacrificing accuracy.

Adapters in other tasks Adapters are extensively studied in parameter-efficient fine-tuning (Houlsby et al., 2019; Rebuffi et al., 2017), which aims to reduce the storage and computational costs associated with adapting pre-trained models to downstream tasks. They typically consist of small, trainable layers within the pre-existing model, while keeping the original parameters frozen. For example, LoRA (Hu et al., 2021) has gained significant attention as a standard method for adapting large language models. Adapters have proven effective across various domains (Stickland & Murray, 2019; Sung et al., 2022; Zhang et al., 2023). While our method shares the same concept of adapters, it is conceptually distinct from prior approaches. Specifically, C-Adapter targets discriminative models by adding an adapter layer to the output layer of the original model, whereas prior adapters consist of trainable mid-layers within the pre-trained model. A key feature of C-Adapter is its ability to preserve the original label ranking, a design specifically tailored for conformal prediction. This distinguishing characteristic sets C-Adapter apart from other adapters.

B VITAL TECHNIQUES IN CONFORMAL PREDICTION

B.1 KEY SCORE FUNCTIONS

Score functions play a crucial role in conformal prediction. With a fixed underlying classifier, the usefulness of the prediction sets is entirely dependent on the chosen score function. Thresholding (THR) (Sadinle et al., 2019) is a commonly used one, which is formulated as:

$$S_{\text{THR}}(\boldsymbol{x}, y; \hat{\pi}) = 1 - \hat{\pi}_y(\boldsymbol{x}).$$

THR tends to generate efficient prediction sets. However, this score function frequently undercovers hard examples while overcovering trivial ones, resulting in high conditional coverage violations.

To mitigate this issue, a popular alternative is the series of adaptive prediction sets. Adaptive Prediction Sets (APS) (Romano et al., 2020), the pioneering work in this series, was specifically designed to reduce conditional coverage violations in classification tasks. It is formulated as follows:

$$S_{\text{APS}}(\boldsymbol{x}, y, u; \hat{\pi}) = \sum_{y_i \in \mathcal{Y}} \hat{\pi}_{y_i}(\boldsymbol{x}) \cdot \mathbb{1}_{\{\hat{\pi}_{y_i}(\boldsymbol{x}) > \hat{\pi}_y(\boldsymbol{x})\}} + u \cdot \hat{\pi}_y(\boldsymbol{x}),$$

where u is an independent random variable following a uniform distribution on $[0,1]$. The prediction set is constructed by adding classes in descending order of probabilities, starting from the most likely to the least, until the cumulative probability exceeds $1-\alpha$.

However, APS always results in large prediction sets since tail classes with low probabilities are easily included. To alleviate this limitation, Regularized Adaptive Prediction Sets (RAPS) (Angelopoulos et al., 2020) penalizes classes based on their rank information with a predefined threshold, thereby promoting the formation of efficient prediction sets. RAPS is formulated as follows:

$$S_{\text{RAPS}}(\boldsymbol{x}, y, u; \hat{\pi}) = S_{\text{APS}}(\boldsymbol{x}, y, u; \hat{\pi}) + \lambda \cdot (o(y, \hat{\pi}(\boldsymbol{x})) - k_{reg})^{+},$$

where $o(y, \hat{\pi}(\boldsymbol{x}))$ is the label ranking of y, λ and k_{reg} are hyperparameters, and $(z)^{+}$ denotes the positive part of z. This regularization encourages more efficient prediction sets. In this work, we evaluate the performance of C-Adapter on THR, APS, and RAPS. For RAPS, we consistently set k_{reg} to 1 and λ to 0.001 across all experiments.

B.2 CONFORMAL TRAINING

The core concept of ConfTr (Stutz et al., 2021) is to render the entire conformal prediction pipeline differentiable, thereby enabling direct optimization of the average prediction set size during classifier training. This process involves simulating both the calibration and prediction phases in each mini-batch. Specifically, mini-batch $\mathcal{B}$ is divided into a calibration subset $\mathcal{B}_{\text{cal}}$ and a test subset $\mathcal{B}_{\text{test}}$. The subset $\mathcal{B}_{\text{cal}}$ is used to compute the soft threshold τ^{soft}, while $\mathcal{B}_{\text{test}}$ is used to obtain the soft prediction sets $\mathcal{C}_{\text{soft}}(\boldsymbol{x}; \tau^{\text{soft}}, \hat{\pi})$ for loss calculations. The detailed operations are as follows:

Soft threshold: During the calibration step, a non-differentiable quantile operation is required to determine the threshold τ. To make this operation differentiable, smooth sorting techniques (Blondel et al., 2020; Cuturi et al., 2019; Williamson, 2020) are employed, as follows:

$$\tau_{\alpha}^{\text{soft}} = \mathcal{Q}_{\text{soft}}(\{S(\boldsymbol{x}, y; \hat{\pi})\}_{(\boldsymbol{x},y)\in\mathcal{B}_{\text{cal}}}, 1-\alpha), \tag{9}$$

where $\mathcal{Q}_{\text{soft}}$ denotes the differentiable quantile operator, derived using smooth sorting techniques.

Soft conformal prediction set: The calculation of conformal prediction sets involves a non-differentiable hard-thresholding operation, as shown in Equation (2). To address this limitation, ConfTr employs the sigmoid function as a differentiable surrogate for the thresholding:

$$\mathcal{C}_{\text{soft}}(\boldsymbol{x}; \tau_{\alpha}^{\text{soft}}, \hat{\pi}) = \left\{ \sigma\left(\frac{\tau_{\alpha}^{\text{soft}} - S(\boldsymbol{x}, y; \hat{\pi})}{T}\right) | y \in \mathcal{Y} \right\}, \tag{10}$$

where σ denotes the sigmoid function and T is a hyperparameter. The k-th term in this set represents a soft assignment of class k, indicating the probability of class k being included in the prediction set. By taking the limit as $T \to 0$, this operator becomes

$$\lim_{T\to 0} \sigma\left(\frac{\tau_{\alpha}^{\text{soft}} - S(\boldsymbol{x}, y; \hat{\pi})}{T}\right) = \begin{cases} 1, & S(\boldsymbol{x}, y; \hat{\pi}) \le \tau_{\alpha}^{\text{soft}}, \\ 0, & S(\boldsymbol{x}, y; \hat{\pi}) > \tau_{\alpha}^{\text{soft}}. \end{cases}$$

For loss calculation, after τ^{soft} is computed using $\mathcal{B}_{\text{cal}}$ as specified in Equation (9), Equation (10) is applied to each instance in $\mathcal{B}_{\text{test}}$ to compute the soft prediction sets. The size of each prediction set is approximated by summing the values in the set $\mathcal{C}_{\text{soft}}(\boldsymbol{x})$, which is optimized during training. Additionally, a standard classification loss, such as cross-entropy loss, is incorporated to enhance classification accuracy. The total loss function is then formulated as follows:

$$\mathcal{L}_{\text{ConfTr}}(f(\boldsymbol{x}; \boldsymbol{\theta}), y, \tau_{\alpha}^{\text{soft}}) = \mathcal{L}_{\text{cls}}(f(\boldsymbol{x}; \boldsymbol{\theta}), y) + \lambda \mathcal{L}_{\text{size}}(f(\boldsymbol{x}; \boldsymbol{\theta}), \tau_{\alpha}^{\text{soft}}),$$

where $\mathcal{L}_{\text{cls}}$ represents the classification loss, and $\mathcal{L}_{\text{size}}$ refers to the size loss, which approximates the size of the prediction set at a specific error rate (e.g., 0.01). Here, λ controls the strength of $\mathcal{L}_{\text{size}}$.

C APPLICATION OF C-ADAPTER

The application of C-Adapter is illustrated in Figure 9. C-Adapter refines the raw logits of trained classifiers for conformal prediction while preserving their intra-order, resulting in more efficient conformal prediction sets without compromising the marginal coverage rate.

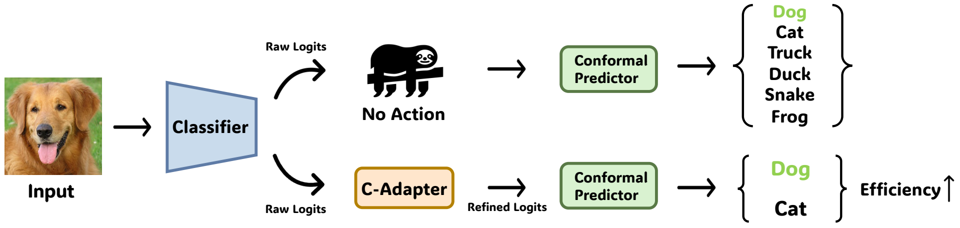

Figure 9: **Application of C-Adapter.** C-Adapter adapts trained classifiers for conformal prediction while preserving the ranking of labels in the output logits. Compared to using the raw logits, this refinement improves the efficiency of prediction sets while maintaining the marginal coverage rate.

D INTRA ORDER-PRESERVING FUNCTIONS

Definition 1. *A function $h : \mathbb{R}^K \to \mathbb{R}^K$ is considered intra order-preserving if, for any vector $\boldsymbol{x} \in \mathbb{R}^K$, the relative ordering of the elements in $\boldsymbol{x}$ is preserved in $h(\boldsymbol{x})$. Formally, $h_i(\boldsymbol{x}) > h_j(\boldsymbol{x})$ (or $h_i(\boldsymbol{x}) = h_j(\boldsymbol{x})$) holds if and only if $\boldsymbol{x}_i > \boldsymbol{x}_j$ (or $\boldsymbol{x}_i = \boldsymbol{x}_j$).*

An intra order-preserving function maintains all ties and inequalities among the input elements. A typical example is the softmax operator presented in Equation (1). The following theorem outlines the necessary and sufficient conditions for constructing continuous intra order-preserving functions.

Theorem 1 (Rahimi et al. (2020))**.** *Let $\mathbb{U}^K \subset \{0,1\}^{K\times K}$ denote the set of $K \times K$ permutation matrices, and let $R : \mathbb{R}^K \to \mathbb{U}^K$ represent the sorting function. For any vector $\boldsymbol{x} \in \mathbb{R}^K$, the vector $\boldsymbol{r} = R(\boldsymbol{x})\boldsymbol{x}$ satisfies $\boldsymbol{r}_1 \geq \cdots \geq \boldsymbol{r}_K$. A continuous function $h : \mathbb{R}^K \to \mathbb{R}^K$ is intra order-preserving if and only if it can be written as $h(\boldsymbol{x}) = R(\boldsymbol{x})^{-1}Ut(\boldsymbol{x})$, where U is an upper-triangular matrix of ones, and $t : \mathbb{R}^K \to \mathbb{R}^K$ is a continuous function that satisfies the following condition: $t_i(\boldsymbol{x}) > 0$ (or $t_i(\boldsymbol{x}) = 0$) if $\boldsymbol{r}_i > \boldsymbol{r}_{i+1}$ (or $\boldsymbol{r}_i = \boldsymbol{r}_{i+1}$), for all $i < K$. The value of $t_K(\boldsymbol{x})$ is arbitrary.*

This theorem provides a pathway for learning within this function family using backpropagation. To maintain the top-k accuracy of the original network, we implement our conformal adapter as a class of intra order-preserving functions, defined as follows:

$$g(\boldsymbol{f};\boldsymbol{w}) = R(\boldsymbol{f})^{-1}U\Psi(\boldsymbol{f}),$$

where the i-th term of $\Psi(\boldsymbol{f})$ is formulated as:

$$\Psi_i(\boldsymbol{f}) = \begin{cases} \sqrt{(\boldsymbol{r}_i - \boldsymbol{r}_{i+1})}\,\sigma(\varphi_i(\boldsymbol{f})) & \text{for } i < K, \\ \varphi_K(\boldsymbol{f}) & \text{for } i = K. \end{cases} \tag{11}$$

Here, $\varphi(\boldsymbol{f}) = \boldsymbol{w} \cdot \boldsymbol{f} + \boldsymbol{w}'$, and σ denotes the sigmoid function. We denote $\varphi_i(\boldsymbol{f})$ as the i-th term of $\varphi(\boldsymbol{f})$. Since $\Psi(\boldsymbol{f})$ is continuous in $\boldsymbol{f}$, it is straightforward to verify that this structure satisfies the requirements outlined in Theorem 1. This structure decouples the logit order from the adaptation for conformal prediction, enabling C-Adapter to focus on optimizing efficiency.

To better demonstrate how this transformation refines input logits for conformal prediction without compromising their ranking, we analyze the algorithm step by step as follows:

1. For an input logit vector $\boldsymbol{f}$, we sort it in descending order. The resulting sorted vector is denoted as $\boldsymbol{r}$, where $\boldsymbol{r}_1 > \boldsymbol{r}_2 > \cdots > \boldsymbol{r}_K$.
2. We calculate $\Psi(\boldsymbol{f})$ using Equation (11). It can be observed that, except for $\Psi_K(\boldsymbol{f})$, if $\boldsymbol{r}_i > \boldsymbol{r}_{i+1}$, this will always result in $\Psi_i(\boldsymbol{f}) > 0$; and if $\boldsymbol{r}_i = \boldsymbol{r}_{i+1}$, it will always result in $\Psi_i(\boldsymbol{f}) = 0$. **Essentially, $\Psi(\boldsymbol{f})$ captures the absolute difference between each element in the transformed logits and the next smaller element.**
3. After calculating $\Psi(\boldsymbol{f})$, we obtain a sorted vector $U\Psi(\boldsymbol{f})$ by performing a reverse cumulative sum operation, where U is an upper-triangular matrix of ones. This sorted vector is denoted as $\boldsymbol{v} = U\Psi(\boldsymbol{f})$. **We observe that $\boldsymbol{v}_i > \boldsymbol{v}_{i+1}$ (or $\boldsymbol{v}_i = \boldsymbol{v}_{i+1}$) holds if and only if $\boldsymbol{r}_i > \boldsymbol{r}_{i+1}$ (or $\boldsymbol{r}_i = \boldsymbol{r}_{i+1}$).** Notably, $\boldsymbol{v}$ is the sorted version of the refined logits.

4. The reverse sorting operator $R(\boldsymbol{f})^{-1}$ is applied to rearrange $\boldsymbol{v}$, aligning it with the order of $\boldsymbol{f}$. This ensures that the resulting vector preserves all ties and inequalities among the input elements. The expressivity of this transformation is guaranteed by the adaptive layer φ.

Notably, to improve convergence and facilitate easier optimization of the structures, we can apply a residual function:

$$g(\boldsymbol{f}; \boldsymbol{w}) = R(\boldsymbol{f})^{-1} U \Psi(\boldsymbol{f}) + \boldsymbol{f}.$$

Additionally, rescaling the input $\boldsymbol{f}$ to the range (0, 1) (e.g., by using the softmax function) can also benefit optimization.

E PROOF FOR PROPOSITION 1

Proof. Considering $(X, Y) \sim \mathcal{P}_{\mathcal{X}\mathcal{Y}}, \hat{X} \sim \mathcal{P}_{\mathcal{X}}, \hat{Y} \sim \text{Uniform}(\mathcal{Y})$, and letting $\mu(\hat{\pi}) := \mathbb{P}\left(S(X, Y; \hat{\pi}) \geq S(\hat{X}, \hat{Y}; \hat{\pi})\right)$, we have

$$\begin{aligned}
\mu(\hat{\pi}) &= \mathbb{E}_{(X,Y)\sim\mathcal{P}_{\mathcal{X}\mathcal{Y}}, \hat{X}\sim\mathcal{P}_{\mathcal{X}}, \hat{Y}\sim\text{Uniform}(\mathcal{Y})} \left[\mathbb{1}_{\{S(X,Y;\hat{\pi}) \geq S(\hat{X},\hat{Y};\hat{\pi})\}}\right] \\
&= \mathbb{E}_{\hat{X}\sim\mathcal{P}_{\mathcal{X}}, \hat{Y}\sim\text{Uniform}(\mathcal{Y})} \left[\mathbb{E}_{(X,Y)\sim\mathcal{P}_{\mathcal{X}\mathcal{Y}}} \left[\mathbb{1}_{\{S(X,Y;\hat{\pi}) \geq S(\hat{X},\hat{Y};\hat{\pi})\}}\right]\right] \\
&= \frac{1}{K} \sum_{\hat{Y}\in\mathcal{Y}} \mathbb{E}_{\hat{X}\sim\mathcal{P}_{\mathcal{X}}} \left[\mathbb{E}_{(X,Y)\sim\mathcal{P}_{\mathcal{X}\mathcal{Y}}} \left[\mathbb{1}_{\{S(X,Y;\hat{\pi}) \geq S(\hat{X},\hat{Y};\hat{\pi})\}}\right]\right] \\
&= \frac{1}{K} \mathbb{E}_{\hat{X}\sim\mathcal{P}_{\mathcal{X}}} \left[\mathbb{E}_{(X,Y)\sim\mathcal{P}_{\mathcal{X}\mathcal{Y}}} \left[\sum_{\hat{Y}\in\mathcal{Y}} \mathbb{1}_{\{S(X,Y;\hat{\pi}) \geq S(\hat{X},\hat{Y};\hat{\pi})\}}\right]\right] \\
&= \frac{1}{K} \mathbb{E}_{\hat{X}\sim\mathcal{P}_{\mathcal{X}}} \left[\mathbb{E}_{s_\theta\sim\mathcal{P}_{S_\theta}} \left[\sum_{\hat{Y}\in\mathcal{Y}} \mathbb{1}_{\{s_\theta \geq S(\hat{X},\hat{Y};\hat{\pi})\}}\right]\right].
\end{aligned}$$

Assuming that the CDF of $\mathcal{P}_\theta$, denoted as F_{S_θ}, is monotonically increasing, we have

$$\begin{aligned}
&\mathbb{E}_{\hat{X}\sim\mathcal{P}_{\mathcal{X}}} \left[\mathbb{E}_{s_\theta\sim\mathcal{P}_{S_\theta}} \left[\sum_{\hat{Y}\in\mathcal{Y}} \mathbb{1}_{\{s_\theta \geq S(\hat{X},\hat{Y};\hat{\pi})\}}\right]\right] \\
&= \mathbb{E}_{\hat{X}\sim\mathcal{P}_{\mathcal{X}}} \left[\int \sum_{\hat{Y}\in\mathcal{Y}} \mathbb{1}_{\{t \geq S(\hat{X},\hat{Y};\hat{\pi})\}} \mathrm{d}F_{S_\theta}(t)\right] \\
(\text{let } t = F_{S_\theta}^{-1}(1-\alpha)) &= \mathbb{E}_{\hat{X}\sim\mathcal{P}_{\mathcal{X}}} \left[\int_1^0 \sum_{\hat{Y}\in\mathcal{Y}} \mathbb{1}_{\{F_{S_\theta}^{-1}(1-\alpha) \geq S(\hat{X},\hat{Y};\hat{\pi})\}} \,\mathrm{d}(1-\alpha)\right] \\
&= \mathbb{E}_{\hat{X}\sim\mathcal{P}_{\mathcal{X}}} \left[\int_0^1 \sum_{\hat{Y}\in\mathcal{Y}} \mathbb{1}_{\{F_{S_\theta}^{-1}(1-\alpha) \geq S(\hat{X},\hat{Y};\hat{\pi})\}} \mathrm{d}\alpha\right] \\
&= \mathbb{E}_{\hat{X}\sim\mathcal{P}_{\mathcal{X}}} \left[\int_0^1 |\mathcal{C}\left(\hat{X}; F_{S_\theta}^{-1}(1-\alpha), \hat{\pi}\right)| \,\mathrm{d}\alpha\right].
\end{aligned}$$

Thus, $\mu(\hat{\pi}) > \mu(\hat{\pi}')$ if and only if

$$\mathbb{E}_{X\sim\mathcal{P}_{\mathcal{X}}} \left[\int_0^1 |\mathcal{C}\left(X; F_{S_\theta}^{-1}(1-\alpha), \hat{\pi}\right)| \,\mathrm{d}\alpha\right] > \mathbb{E}_{X\sim\mathcal{P}_{\mathcal{X}}} \left[\int_0^1 |\mathcal{C}\left(X; F_{S_\theta}^{-1}(1-\alpha), \hat{\pi}'\right)| \,\mathrm{d}\alpha\right].$$

□

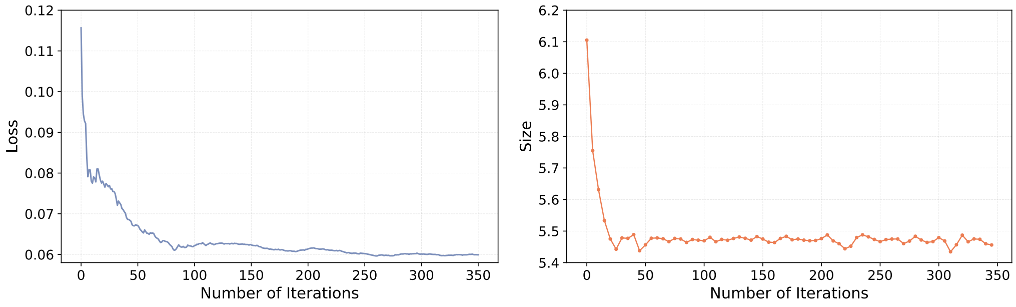

(a) Loss (b) Size of THR

Figure 10: Convergence analysis of C-Adapter on ImageNet using DN121.

F CONVERGENCE ANALYSIS

Our method is computationally efficient as it updates only a limited number of parameters and can converge rapidly. To demonstrate this, we conduct an experiment on ImageNet using DN121, visualizing the changes in loss and efficiency over iterations. We tune C-Adapter with Adam, using a learning rate of 0.1, a batch size of 256, and a weight decay of 0.0001. We apply THR during adapter tuning. We also use THR for evaluation and set the error rate to 0.5. As shown in Figure 10, our method converges rapidly within **200 iterations**, with the efficiency of the conformal predictor improving quickly and approaching nearly optimal performance in just **50 iterations**. This convergence analysis highlights the computational efficiency of our proposed approach.

G EVALUATION METRICS

Size refers to the average number of labels in the prediction sets, while Coverage indicates the percentage of test samples where the prediction sets contain the ground-truth labels:

$$\text{Size} = \frac{1}{|\mathcal{D}_{\text{test}}|} \sum_{(\boldsymbol{x},y)\in\mathcal{D}_{\text{test}}} |\mathcal{C}(\boldsymbol{x})|,$$

$$\text{Coverage} = \frac{1}{|\mathcal{D}_{\text{test}}|} \sum_{(\boldsymbol{x},y)\in\mathcal{D}_{\text{test}}} \mathbb{1}_{\{y\in\mathcal{C}(\boldsymbol{x})\}}.$$

CovGap (Ding et al., 2024) and SSCV (Angelopoulos et al., 2020) are defined as follows:

$$\text{CovGap} = 100 \times \frac{1}{|\mathcal{Y}|} \sum_{y\in\mathcal{Y}} |\hat{c}_y - (1-\alpha)|,$$

$$\text{SSCV} = 100 \times \sup_j \left| (1-\alpha) - \frac{|\{i : y_i \in \mathcal{C}(\boldsymbol{x}_i), i \in \mathcal{J}_j\}|}{|\mathcal{J}_j|} \right|.$$

For CovGap, $\hat{c}_y$ denotes the coverage rate for class y and quantifies the deviation of class-conditional coverage from the desired level of $1-\alpha$. For SSCV, $\mathcal{J}$ represents the partitioned sets, with the prediction sets categorized by their sizes. This metric evaluates the maximum deviation of the observed coverage rate from $1-\alpha$ across different set size categories. In our experiment, the partitioning of set sizes for SSCV is defined as {0-1, 2, 3, 4, 5, 6, 7, 8, 9, 10, 11-100, 101-1000}.

H DETAILED EXPERIMENTAL SETUP

H.1 DETAILED SETUP FOR FIGURE 1

For CIFAR100, ResNet18 is trained using the full training set of 50,000 samples. The test set of 10,000 samples is divided into a calibration subset of 5,000 samples and a test subset of 5,000 samples. The calibration subset is further split into a validation set and a calibration set in an 20:80 ratio for parameter tuning. The network is trained for 200 epochs using SGD with a momentum of

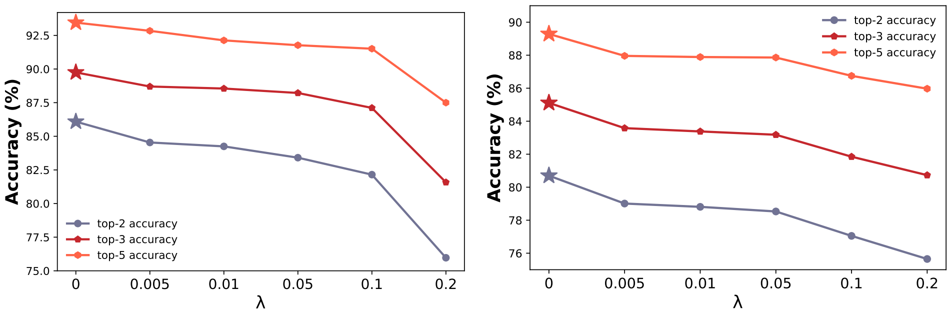

(a) CIFAR100

(b) ImageNet

Figure 11: **The accuracy of ConfTr with various $\boldsymbol{\lambda}$**, using ResNet18 on (a) CIFAR-100 and (b) ImageNet. ★ denotes the baseline without ConfTr. The results indicate that increasing λ consistently decreases the top-2, top-3, and top-5 classification accuracies.

0.9, a weight decay of 0.0005, and a batch size of 256. The initial learning rate is set to 0.1 and is reduced by a factor of 5 at 60, 120, and 160 epochs. The hyperparameters T and λ of ConfTr are tuned from the ranges $\{0.01, 0.1, 0.5, 1\}$ and $\{0.005, 0.01, 0.05, 0.1, 0.2\}$, respectively.

For ImageNet, instead of training from scratch, we fine-tune only the fully connected layer of a pre-trained ResNet18 using the training set. The test set is divided into a calibration subset of 30,000 samples and a test subset of 20,000 samples, with the calibration subset further split into a validation set and a calibration set in a 20:80 ratio for parameter tuning. The fully connected layer is tuned for 240 iterations using Adam with a batch size of 256 and a learning rate of 0.001. A larger learning rate significantly decreases classification accuracy, thereby reducing efficiency. The hyperparameters T and λ for ConfTr are selected from the ranges $\{0.01, 0.1, 0.5, 1\}$ and $\{0.001, 0.005, 0.01, 0.05, 0.1\}$, respectively; a larger λ also leads to a substantial decline in accuracy.

For evaluation, we use THR, APS, and RAPS, with the error rate α set to 0.1. During model training, we utilize the THRLP score function (Stutz et al., 2021), setting the error rate α to 0.01. We also present the top-2, top-3, and top-5 accuracy of ConfTr on CIFAR100 and ImageNet in Figure 11.

H.2 DETAILED SETUP FOR FIGURE 5

Retraining: Classifiers are trained using the complete training set of 50,000 samples, with the objective defined in Equation (7). The network is trained for 200 epochs using SGD with a momentum of 0.9, a weight decay of 0.0005, and a batch size of 256. The initial learning rate is set to 0.1 and reduced by a factor of 5 at epochs 60, 120, and 160. The parameter T is tuned within the range $\{0.001, 0.01, 0.1, 1\}$ using the validation set. We utilize THR for classifier training.

Fine-tuning: Classifiers are trained using the same training set of 50,000 samples with cross-entropy loss. The network is trained for 200 epochs using SGD, with a momentum of 0.9, a weight decay of 0.0005, and a batch size of 256. The initial learning rate is set to 0.1, reduced by a factor of 5 at epochs 60, 120, and 160. During fine-tuning, only the fully connected layer of the pre-trained classifier is updated, training for 240 iterations with Adam, a batch size of 256, and a learning rate of 0.001. Notably, a larger learning rate results in a significant decrease in classification accuracy. The parameter T is tuned from the range $\{0.001, 0.01, 0.1, 1\}$ using the validation set.

I ADDITIONAL EXPERIMENTAL RESULTS

Results when tuning C-Adapter using APS We report the detailed results of Coverage and Size when C-Adapter is tuned using APS. Empirical results in Table 5 demonstrate that C-Adapter consistently enhances the efficiency of conformal predictors, regardless of the model architectures and pre-training strategies, highlighting the flexibility of our approach.

Table 5: **Performance of C-Adapter on common benchmarks.** ↓ indicates that a smaller value is better. Results in **bold** indicate superior performance. C-Adapter is tuned using APS.

Score	Model	w/o C-Adapter \ w/ C-Adapter							
		ImageNet				**CIFAR-100**			
		$\alpha = 0.05$		$\alpha = 0.1$		$\alpha = 0.05$		$\alpha = 0.1$	
		Coverage	Size (↓)	Coverage	Size (↓)	Coverage	Size (↓)	Coverage	Size (↓)
THR	RN101	0.95 \ 0.95	4.03 \ **3.66**	0.90 \ 0.90	1.91 \ **1.86**	0.95 \ 0.95	3.64\ **3.11**	0.90 \ 0.90	1.87 \ **1.80**
	DN121	0.95 \ 0.95	5.66 \ **5.39**	0.90 \ 0.90	2.42 \ **2.40**	0.95 \ 0.95	3.27 \ **3.03**	0.90 \ 0.90	1.72 \ **1.69**
	DN161	0.95 \ 0.95	4.03 \ **3.88**	0.90 \ 0.90	1.89 \ **1.86**	0.95 \ 0.95	2.91 \ **2.71**	0.90 \ 0.90	1.72 \ **1.71**
	RNX50	0.95 \ 0.95	4.26 \ **3.93**	0.90 \ 0.90	1.87 \ **1.84**	0.95 \ 0.95	3.41 \ **3.16**	0.90 \ 0.90	1.78 \ **1.77**
	CLIP	0.95 \ 0.95	**6.88** \ 6.90	0.90 \ 0.90	3.33 \ **3.28**	0.95 \ 0.95	9.71\ **9.67**	0.90 \ 0.90	4.78 \ **4.69**
	Average	0.95 \ 0.95	4.97 \ **4.75**	0.90 \ 0.90	2.29 \ **2.25**	0.95 \ 0.95	4.59 \ **4.34**	0.90 \ 0.90	2.37 \ **2.33**
APS	RN101	0.95 \ 0.95	14.73 \ **3.82**	0.90 \ 0.90	7.23 \ **2.07**	0.95 \ 0.95	7.60 \ **3.16**	0.90 \ 0.90	3.95 \ **1.80**
	DN121	0.95 \ 0.95	20.00 \ **5.64**	0.90 \ 0.90	9.21 \ **2.74**	0.95 \ 0.95	10.20 \ **4.12**	0.90 \ 0.90	4.44 \ **2.35**
	DN161	0.95 \ 0.95	16.43 \ **4.13**	0.90 \ 0.90	6.82 \ **2.05**	0.95 \ 0.95	9.90 \ **3.14**	0.90 \ 0.90	5.42 \ **1.87**
	RNX50	0.95 \ 0.95	21.54 \ **4.10**	0.90 \ 0.90	8.92 \ **2.07**	0.95 \ 0.95	9.95 \ **3.19**	0.90 \ 0.90	5.14 \ **1.90**
	CLIP	0.95 \ 0.95	26.35 \ **7.42**	0.90 \ 0.90	13.24 \ **3.43**	0.95 \ 0.95	16.13 \ **12.94**	0.90 \ 0.90	10.18 \ **8.10**
	Average	0.95 \ 0.95	19.81 \ **5.04**	0.90 \ 0.90	9.08 \ **2.47**	0.95 \ 0.95	10.76 \ **5.31**	0.90 \ 0.90	6.01 \ **3.20**
RAPS	RN101	0.95 \ 0.95	7.13 \ **4.43**	0.90 \ 0.90	4.60 \ **2.01**	0.95 \ 0.95	5.16 \ **4.71**	0.90 \ 0.90	3.25 \ **1.81**
	DN121	0.95 \ 0.95	10.28 \ **7.38**	0.90 \ 0.90	6.57 \ **2.66**	0.95 \ 0.95	7.19\ **4.00**	0.90 \ 0.90	4.50 \ **1.83**
	DN161	0.95 \ 0.95	7.31 \ **5.01**	0.90 \ 0.90	4.63 \ **2.00**	0.95 \ 0.95	7.10 \ **3.22**	0.90 \ 0.90	4.59 \ **1.81**
	RNX50	0.95 \ 0.95	7.88 \ **5.05**	0.90 \ 0.90	5.20 \ **2.01**	0.95 \ 0.95	7.20 \ **3.64**	0.90 \ 0.90	4.47 \ **1.79**
	CLIP	0.95 \ 0.95	15.14 \ **8.74**	0.90 \ 0.90	9.25 \ **3.41**	0.95 \ 0.95	14.52 \ **13.61**	0.90 \ 0.90	9.41 \ **8.92**
	Average	0.95 \ 0.95	9.55 \ **6.12**	0.90 \ 0.90	6.05 \ **2.42**	0.95 \ 0.95	8.24 \ **5.84**	0.90 \ 0.90	5.24 \ **3.23**

Table 6: **Robustness of C-Adapter under different data shifts.** C-Adapter is tuned using ImageNet and tested on ImageNet-R and ImageNet-A. The base classifier adopted in this experiment is RN101. Since each entry achieves the desired coverage, only **Size** is presented.

Dataset	w/o C-Adapter \ w/ C-Adapter					
	THR		**APS**		**RAPS**	
	$\alpha = 0.4$	$\alpha = 0.5$	$\alpha = 0.4$	$\alpha = 0.5$	$\alpha = 0.4$	$\alpha = 0.5$
ImageNet-R	6.13 \ **5.56**	2.23 \ **2.11**	11.32 \ **7.16**	6.16 \ **2.61**	6.24 \ **5.95**	3.32 \ **2.78**
ImageNet-A	26.99 \ **20.09**	18.21 \ **13.13**	36.62 \ **23.01**	25.98 \ **17.56**	20.26 \ **20.08**	13.72 \ **13.40**
Average	16.56 \ **13.25**	10.22 \ **7.62**	23.97 \ **15.09**	16.07 \ **10.09**	13.25 \ **13.02**	8.52 \ **8.09**

C-Adapter is robust to various distribution shifts. We further investigate the robustness of C-Adapter on ImageNet-R(rendition) (Hendrycks et al., 2021a) and ImageNet-A(adversarial) (Hendrycks et al., 2021b). ImageNet-A and ImageNet-R are extended versions of the ImageNet dataset designed to evaluate model robustness, with ImageNet-A focusing on adversarial examples that are modified to mislead models, and ImageNet-R consisting of images transformed by various artistic styles and visual changes to test models' adaptability to different visual distributions.

Specifically, we fine-tune C-Adapter using the ImageNet training set, then split both ImageNet-R and ImageNet-A into equal-sized calibration and test sets for conformal prediction. In this experiment, we use pre-trained RN101. Given the relatively low performance of the pre-trained RN101 on ImageNet-R and ImageNet-A (for example, it achieves only 39% classification accuracy on ImageNet-R), we set the error rate α to 0.4 and 0.5, respectively. Notably, coverage remains unaffected by this setting, as the calibration and test sets are still exchangeable. We evaluate the performance of C-Adapter using the APS, THR, and RAPS. As shown in Table 6, C-Adapter consistently reduces size across various base classifiers on both ImageNet-R and ImageNet-A, regardless of the score function used in conformal prediction or the predefined error rate α. The experimental results further highlight the robustness of C-Adapter under different kinds of data shift.

Results on text classification using LLMs To provide a comprehensive understanding of the broad capabilities of our method, we evaluate its performance on a text classification task. Additionally, we demonstrate the versatility of C-Adapter by performing this task using Large Language Models (LLMs). Before delving into the experiment, we introduce a commonly used framework for

Table 7: **Performance of C-Adapter on text classification.** ↓ indicates that a smaller value is better. C-Adapter is tuned using THR. The experiment is carried on dbpedia_14 using LLama3-8B.

Score	**w/o C-Adapter \ w/ C-Adapter**			
	$\alpha = 0.05$		$\alpha = 0.1$	
	Coverage	Size (↓)	Coverage	Size (↓)
THR	0.94 \ 0.95	2.80 \ **2.61**	0.89 \ 0.89	2.17 \ **2.04**
APS	0.95 \ 0.94	3.14 \ **2.75**	0.90 \ 0.91	2.33 \ **2.08**
RAPS	0.95 \ 0.95	3.23 \ **3.11**	0.90 \ 0.90	2.48 \ **2.32**
Average	–	3.06 \ **2.82**	–	2.33 \ **2.15**

applying LLMs to text classification. For each input, we construct a prompt in the following format:

```
\n Company, Educational Institution, Artist, Athlete, Office
    Holder, Mode of Transportation, Building, Natural Place,
    Village, Animal, Plant, Album, Film, or Written Work? \n Input
    : </text> \n Output: </text>
```

In this prompt, each input instance $\boldsymbol{x}$ is paired with a label $y \in \mathcal{Y}$, where $\mathcal{Y}$ represents the set of possible categories (e.g., ”Company”, ”Artist”, etc.). The input $\boldsymbol{x}$ and label y are then inserted into the appropriate position in the prompt. After obtaining the model's output, we construct the input-output pair $\boldsymbol{z}$, tokenize it, and calculate its perplexity as follows:

$$\text{Perplexity}(\boldsymbol{z}) = \exp\left(-\frac{1}{N}\sum_{i=1}^{N}\log p(z_i|z_{<i})\right),$$

where $p(z_i|z_{<i})$ denotes the predicted probability of token z_i given the preceding tokens, and N is the total number of tokens in the input-output pair $\boldsymbol{z}$. Perplexity quantifies the uncertainty of the language model in predicting the next token in the sequence. The label corresponding to the input-output pair $\boldsymbol{z}$ with the lowest perplexity is selected as the predicted label for the input $\boldsymbol{x}$.

We perform conformal prediction in this classification setting, specifically on the `dbpedia_14` dataset, a 14-class classification task (Lehmann et al., 2015). For the LLM, we use LLama3-8B (Touvron et al., 2023). In this experiment, we apply conformal prediction based on perplexity. For an input $\boldsymbol{x}$, we compute the perplexity vector for each label $y \in \mathcal{Y}$. Since a lower perplexity indicates a more likely label, the reciprocal of the normalized perplexity is used as the raw logits to perform conformal prediction. We use the test set of `dbpedia_14` with 7,480 samples to perform the experiment, where 2,000 of them are used for tuning, and the remaining data is equally and randomly divided into calibration and test sets. Notably, we rely on the zero-shot ability of LLama3-8B to perform classification. The classification accuracy on this set is 66%. The experimental results are presented in Table 7. Compared to using the raw perplexity as input logits, C-Adapter significantly improves the efficiency of conformal prediction across different conditions.

Comparison of different surrogate functions for the indicator function In this section, we compare the performance of C-Adapter using different surrogate functions for the indicator function within its loss function, with all experimental settings kept constant. Specifically, we investigate three widely used surrogate functions, as follows:

- Hinge: $h(x) = \max(x + c, 0)$, where c is a parameter.
- Square: $s(x) = (x + c)^2$, where c is a parameter.
- Sigmoid: $\sigma(x) = \frac{1}{1+\exp(-x/T)}$, where T is a parameter.

For parameter tuning, we fix the parameter T of the Sigmoid function at 0.0001, while the parameters of the Hinge and Square functions are tuned using grid search with a step size of 0.2 over the interval $[0, 1]$. The error rate α is set to 0.05, and the results are presented in Table 8. As observed, the Sigmoid function outperforms the others regardless of the applied score function.

Table 8: **Comparison of loss functions with different surrogate functions,** on ImageNet with DN121. Baseline represents the scenario without C-Adapter. Since all methods achieve the desired coverage, only **Size** is reported. The Sigmoid function outperforms the other surrogate functions.

	Baseline	Hinge	Square	Sigmoid
THR	5.66	5.51	5.47	**5.41**
APS	20.00	5.91	5.88	**5.73**
RAPS	10.28	7.49	7.35	**6.53**
Average	11.98	6.30	6.23	**5.89**

J ANALYSIS OF CONDITIONAL COVERAGE

In this section, we analyze why C-Adapter can improve the conditional coverage metrics, i.e., CovGap and SSCV. For a trained classifier, large values of SSCV and CovGap typically stem from significant performance variations across sub-groups of data, which cause disparities in non-conformity scores between groups. When a single threshold τ is applied to generate prediction sets for these sub-groups, the resulting conditional coverage gaps can become substantial. In this section, we show that, from a gradient perspective, our loss function mitigates these discrepancies by reducing the variation in non-conformity scores across samples. This reduction leads to more uniform performance across different sub-groups, ultimately improving conditional coverage metrics. For any sample $(\boldsymbol{x}, y)$ from batch $\mathcal{B}$, the corresponding loss is calculate by

$$\mathcal{L}(\boldsymbol{x}, y) = \frac{1}{|\hat{B}|} \sum_{(\hat{\boldsymbol{x}}, \hat{y}) \in \hat{\mathcal{B}}} \sigma\left(\frac{S(\boldsymbol{x}, y; \widetilde{\pi}_{\boldsymbol{w}}) - S(\hat{\boldsymbol{x}}, \hat{y}; \widetilde{\pi}_{\boldsymbol{w}})}{T}\right).$$

Let $\Delta(\hat{\boldsymbol{x}}, \hat{y})$ denote the difference between the scores for $(\boldsymbol{x}, y)$ and $(\hat{\boldsymbol{x}}, \hat{y})$ as:

$$\Delta(\hat{\boldsymbol{x}}, \hat{y}) = S(\boldsymbol{x}, y; \widetilde{\pi}_{\boldsymbol{w}}) - S(\hat{\boldsymbol{x}}, \hat{y}; \widetilde{\pi}_{\boldsymbol{w}}).$$

Additionally, let $S = S(\boldsymbol{x}, y; \widetilde{\pi}_{\boldsymbol{w}})$ represent the score for $(\boldsymbol{x}, y)$. Then, we have

$$\frac{\partial \mathcal{L}(\boldsymbol{x}, y)}{\partial S} = \frac{1}{|\hat{\mathcal{B}}|} \frac{1}{T} \sum_{(\hat{\boldsymbol{x}}, \hat{y}) \in \hat{\mathcal{B}}} \sigma\left(\frac{\Delta(\hat{\boldsymbol{x}}, \hat{y})}{T}\right)\left(1 - \sigma\left(\frac{\Delta(\hat{\boldsymbol{x}}, \hat{y})}{T}\right)\right).$$

We observe that the magnitude of $\frac{\partial \mathcal{L}(\boldsymbol{x}, y)}{\partial S}$ is determined by $\Delta(\hat{\boldsymbol{x}}, \hat{y})$. Specifically, the gradient's magnitude decreases as $\Delta(\hat{\boldsymbol{x}}, \hat{y})$ moves further from zero. Since T is typically small, the value decreases rapidly. We now analyze the gradient's magnitude in two different cases:

- If S is low and well separated from the scores of randomly matched samples $S(\hat{\boldsymbol{x}}, \hat{y}; \widetilde{\pi}_{\boldsymbol{w}})$, then $\Delta(\hat{\boldsymbol{x}}, \hat{y})$ will typically be negative, and its absolute value will be large in most cases. As a result, the magnitude of the corresponding gradient will be extremely low.
- If S is high and cannot be easily distinguished from the scores of randomly matched samples $S(\hat{\boldsymbol{x}}, \hat{y}; \widetilde{\pi}_{\boldsymbol{w}})$, then $\Delta(\hat{\boldsymbol{x}}, \hat{y})$ will approach zero for many $(\hat{\boldsymbol{x}}, \hat{y}) \in \hat{\mathcal{B}}$, resulting in a large gradient magnitude. This encourages the reduction of such high scores.

This characteristic rebalances the learning process by placing greater emphasis on samples with high non-conformity scores (hard-to-distinguish score), and thus reducing the variation in non-conformity scores across samples. Consequently, the model achieves more consistent performance across different data subgroups, ultimately enhancing conditional coverage metrics.

K THEORETICAL ANALYSIS OF THE IMPACT OF CLASSIFICATION ACCURACY ON THE EFFICIENCY OF CONFORMAL PREDICTORS

In Figures 1 and 11, we have empirically shown that ConfTr reduces the top-k accuracy of classifiers. In this section, we formally analyze how top-k accuracy affects the efficiency of conformal predictors. The following propositions demonstrate that the lower and upper bounds of the expected size of the prediction set at level $1-\alpha$ are related to the top-k accuracy of the classifier. For notation shorthand, given the classifier $\hat{\pi}$, we define $o(y) \equiv o(y, \hat{\pi}(\boldsymbol{x}; \boldsymbol{\theta}))$ to denote the index of label y in the sorted softmax probabilities for $\boldsymbol{x} \sim \mathcal{P}_{\mathcal{X}}$.

Proposition 2 (Lower bound)**.** *Let $\hat{\pi}$ be a classifier with top-J classification accuracy acc_J, and let the error rate be α. Then, the expected size of the conformal prediction set is bounded below by:*

$$\mathbb{E}\left[|\mathcal{C}(X)|\right] \geq \begin{cases} (J+1)(1-\alpha) - J \cdot acc_J, & \text{if } acc_J \leq 1-\alpha, \\ 1-\alpha, & \text{if } acc_J > 1-\alpha. \end{cases}$$

The proof is provided in Appendix K.1. According to Proposition 2, **the lower bound of the expected set size is negatively related to the top-k accuracy**. Therefore, the cost of accuracy introduced by ConfTr will increase the lower bound of the expected size, leading to suboptimal performance in efficiency. This highlights the importance of preserving top-k accuracy in the efficiency optimization for conformal prediction.

Proposition 3 (Upper bound)**.** *Let $\hat{\pi}$ be a classifier with top-J classification accuracy acc_J, and let the error rate be α. Then, the expected size of the conformal prediction set is bounded above by:*

$$\mathbb{E}\left[|\mathcal{C}(X)|\right] \leq K - 1 - (K-J)acc_J + \mathbb{E}\left[\sum_{\hat{Y}\in\mathcal{Y}} t(X,Y,\hat{Y})\right],$$

where $(X,Y) \sim \mathcal{P}_{\mathcal{X}\mathcal{Y}}, t(X,Y,\hat{Y}) = \mathbb{1}\{\{S(X,\hat{Y}) \leq \tau_\alpha\} \cap \{o(Y) < o(\hat{Y})\} \cap \{Y \in \mathcal{C}(X)\}\}$.

The proof is provided in Appendix K.2. According to Proposition 3, the average set size at error rate α is upper bounded by two terms. The first term is negatively related to the top-k accuracy. The second term in this bound represents the expected number of labels $\hat{Y}$ that satisfy the condition:

$$\{S(X,\hat{Y}) \leq \tau_\alpha\} \cap \{o(Y) < o(\hat{Y})\} \cap \{Y \in \mathcal{C}(X)\},$$

over $(X,Y) \sim \mathcal{P}_{\mathcal{X}\mathcal{Y}}$. This expectation primarily reflects the number of incorrect labels that have non-conformity scores lower than τ_α and are ranked higher than the true label Y. Intuitively, a drop in model performance reduces the discriminative ability, making it harder to distinguish between correct and incorrect labels. As a result, correct and incorrect labels may have similar scores, which can lead to an increase in the value of the second term. These analyses highlight the negative impact of decreased model performance on the efficiency of conformal predictors.

K.1 PROOF OF PROPOSITION 2

Proof. To obtain the lower bound of the expected set size, we assume an oracle score function and an ideal model such that, for the case $\text{acc}_J \leq 1-\alpha$:

$$|\mathcal{C}^*(X)| = \begin{cases} 0, & \text{if } Y \notin \mathcal{C}(X), \\ 1, & \text{if } o(Y) \leq J \text{ and } Y \in \mathcal{C}(X), \\ J+1, & \text{if } o(Y) > J \text{ and } Y \in \mathcal{C}(X), \end{cases}$$

where $(X,Y) \sim \mathcal{P}_{\mathcal{X}\mathcal{Y}}$.

Given the top-J accuracy acc_J, to satisfy the desired coverage rate of $1-\alpha$, the expected value of minimal set size is:

$$\begin{aligned} \mathbb{E}[C^*(X)] &= \text{acc}_J \cdot 1 + (1-\alpha-\text{acc}_J)(J+1) + (1-\alpha)\cdot 0 \\ &= (J+1)(1-\alpha) - J \cdot \text{acc}_J. \end{aligned}$$

Thus, we have the lower bound in the case $\text{acc}_J \leq 1-\alpha$:

$$\mathbb{E}[C(X)] \geq (J+1)(1-\alpha) - J \cdot \text{acc}_J.$$

Similarly, for the case $\text{acc}_J > 1-\alpha$, we have:

$$|\mathcal{C}^*(X)| = \begin{cases} 0, & \text{if } Y \notin \mathcal{C}(X), \\ 1, & \text{if } o(Y) \leq J \text{ and } Y \in \mathcal{C}(X), \end{cases}$$

where $(X, Y) \sim \mathcal{P}_{\mathcal{X}\mathcal{Y}}$.

In this case, the minimal size of expected prediction sets under the top-J accuracy acc_J is:

$$\mathbb{E}[C^*(X)] = (1-\alpha)(1) + \alpha \cdot 0 = 1 - \alpha.$$

Therefore, we have the lower bound in the case $\text{acc}_J > 1 - \alpha$:

$$\mathbb{E}[C(X)] \geq 1 - \alpha.$$

Now we have the lower bound of the expected set size:

$$\mathbb{E}\left[|\mathcal{C}(X)|\right] \geq \begin{cases} (J+1)(1-\alpha) - J \cdot \text{acc}_J, & \text{if } \text{acc}_J \leq 1-\alpha, \\ 1-\alpha, & \text{if } \text{acc}_J > 1-\alpha. \end{cases}$$

□

K.2 PROOF OF PROPOSITION 3

Proof. For notation shorthand, we denote $\mathbb{E}_{(X,Y)\sim\mathcal{P}_{\mathcal{X}\mathcal{Y}}}\left[|\mathcal{C}(X)|\right]$ as $\mathbb{E}\left[|\mathcal{C}(X)|\right]$. We can decompose $\mathbb{E}\left[|\mathcal{C}(X)|\right]$ based on whether $\mathcal{C}(X)$ contains the true label Y as

$$\mathbb{E}\left[|\mathcal{C}(X)|\right] = \underbrace{\mathbb{E}\left[|\mathcal{C}(X)|\,|Y \in \mathcal{C}(X)\right]}_{(a)} \cdot \mathbb{P}\left\{Y \in \mathcal{C}(X)\right\} + \underbrace{\mathbb{E}\left[|\mathcal{C}(X)|\,|Y \notin \mathcal{C}(X)\right]}_{(b)} \cdot \mathbb{P}\left\{Y \notin \mathcal{C}(X)\right\}.$$

We analyze the two parts individually, as follows:

Part (a): For prediction sets containing the ground truth, we have:

$$\begin{aligned}
&\mathbb{E}\left[|\mathcal{C}(X)|\,|Y \in \mathcal{C}(X)\right] = \mathbb{E}\left[\sum_{\hat{Y}\in\mathcal{Y}} \mathbb{1}\{S(X,\hat{Y}) \leq \tau_\alpha\} \mid Y \in \mathcal{C}(X)\right] \\
&= \mathbb{E}\left[\sum_{\hat{Y}\in\mathcal{Y}} \mathbb{1}\{o(Y) \geq o(\hat{Y})\} \cdot \mathbb{1}\{S(X,\hat{Y}) \leq \tau_\alpha\} + \sum_{\hat{Y}\in\mathcal{Y}} \mathbb{1}\{o(Y) < o(\hat{Y})\} \cdot \mathbb{1}\{S(X,\hat{Y}) \leq \tau_\alpha\} | Y \in \mathcal{C}(X)\right] \\
&\overset{(1)}{=} \mathbb{E}\left[o(Y) + \sum_{\hat{Y}\in\mathcal{Y}} \mathbb{1}\{o(Y) < o(\hat{Y})\} \cdot \mathbb{1}\{S(X,\hat{Y}) \leq \tau_\alpha\} | Y \in \mathcal{C}(X)\right] \\
&= \mathbb{E}\left[o(Y) | Y \in \mathcal{C}(X)\right] + \sum_{\hat{Y}\in\mathcal{Y}} \mathbb{P}\left\{S(X,\hat{Y}) \leq \tau_\alpha, o(Y) < o(\hat{Y}) \mid Y \in \mathcal{C}(X)\right\}
\end{aligned}$$

where (1) holds because under the condition $Y \in \mathcal{C}(X)$, we have $\mathbb{1}\{S(X,\hat{Y}) \leq \tau\} = 1$ for all label $y \in \mathcal{Y}$ satisfying $o(\hat{Y})) \leq o(Y)$.

Part (b): It is obvious to obtain that, for prediction sets that do not contain the ground truth, the size is bounded by the label order of the ground truth minus one, as follows:

$$\mathbb{E}\left[|\mathcal{C}(X)| \mid Y \notin \mathcal{C}(X)\right] \leq \mathbb{E}\left[o(Y) \mid Y \notin \mathcal{C}(X)\right] - 1.$$

Combining the results from **Part (a)** and **Part (b)** gives

$$\begin{aligned}
\mathbb{E}\left[|\mathcal{C}(X)|\right] \leq &\,\mathbb{E}\left[o(Y) | Y \notin \mathcal{C}(X)\right] \cdot \mathbb{P}\left\{Y \notin \mathcal{C}(X)\right\} + \mathbb{E}\left[o(Y) | Y \in \mathcal{C}(X)\right] \cdot \mathbb{P}\left\{Y \in \mathcal{C}(X)\right\} + \\
&\sum_{\hat{Y}\in\mathcal{Y}} \mathbb{P}\left\{S(X,\hat{Y}) \leq \tau_\alpha, o(Y) < o(\hat{Y}), Y \in \mathcal{C}(X)\right\} - 1 \\
= &\,\mathbb{E}[o(Y)] + \mathbb{E}\left[\sum_{\hat{Y}\in\mathcal{Y}} \mathbb{1}\{(S(X,\hat{Y}) \leq \tau_\alpha) \cap (o(Y) < o(\hat{Y})) \cap (Y \in \mathcal{C}(X))\}\right] - 1.
\end{aligned}$$

And for a pre-specified Top-J accuracy, acc_J, we have

$$\begin{aligned}\mathbb{E}[o(Y)] =& \sum_{k=1}^{K} k\mathbb{P}(o(Y) = k) \\ =& \sum_{k=1}^{J} k\mathbb{P}(o(Y) = k) + \sum_{k=J+1}^{K} k\mathbb{P}(o(Y) = k) \\ \leq& J\mathrm{acc}_J + K(1 - \mathrm{acc}_J) \\ =& K - (K - J)\mathrm{acc}_J.\end{aligned}$$

□